



Radio Astronomical Tools for the Study of Solar Energetic Particles II. Time-Extended Acceleration at Subrelativistic and Relativistic Energies

Karl-Ludwig Klein *

Observatoire de Paris, LESIA & Station de Radioastronomie de Nançay, University PSL, CNRS, Sorbonne University, University of Paris, University D'Orléans, Meudon, France

OPEN ACCESS

Edited by:

Dale E. Gary,
New Jersey Institute of Technology,
United States

Reviewed by:

Ian Richardson,
University of Maryland, United States
Abhishek Kumar Srivastava,
Indian Institute of Technology (BHU),
India

*Correspondence:

Karl-Ludwig Klein
ludwig.klein@obsprm.fr

Specialty section:

This article was submitted to
Stellar and Solar Physics,
a section of the journal
Frontiers in Astronomy and Space
Sciences

Received: 06 July 2020

Accepted: 27 October 2020

Published: 11 March 2021

Citation:

Klein K-L (2021) Radio Astronomical Tools for the Study of Solar Energetic Particles II. Time-Extended Acceleration at Subrelativistic and Relativistic Energies. *Front. Astron. Space Sci.* 7:580445. doi: 10.3389/fspas.2020.580445

Solar energetic particle (SEP) events are commonly separated in two categories: numerous “impulsive” events of relatively short duration, and a few “gradual” events, where SEP-intensities may stay enhanced over several days at energies up to several tens of MeV. In some gradual events the SEP spectrum extends to relativistic energies (> 1 GeV), over shorter durations. The two categories are strongly related to an idea developed in the 1960s based on radio observations: Type III bursts, which were addressed in a companion chapter, outline impulsive acceleration of electrons to subrelativistic energies, while the large and the relativistic SEP events were ascribed to a second acceleration process. At radio wavelengths, typical counterparts were bursts emitted by electrons accelerated at coronal shock waves (type II bursts) and by electron populations in large-scale closed coronal structures (type IV bursts). Both burst types are related to coronal mass ejections (CMEs). Type II bursts from metric to kilometric wavelengths tend to accompany large SEP events, which is widely considered as a confirmation that CME-driven shocks accelerate the SEPs. But type II bursts, especially those related to SEP events, are most often accompanied by type IV bursts, where the electrons are rather accelerated in the wake of the CME. Individual event studies suggest that although the CME shock is the most plausible accelerator of SEPs up to some yet unknown limiting energy, the relativistic SEP events show time structure that rather points to coronal acceleration related to type IV bursts. This chapter addresses the question what type II bursts tell us about coronal shock waves and how type II and type IV radio bursts are related with relativistic proton signatures as seen by particle detectors on the Earth and by their gamma-ray emission in the solar atmosphere, focusing on two relativistic SEP events, on 2005 Jan 20 and 2017 Sep 10. The importance of radio emissions as a complement to the upcoming SEP observations from close to the Sun is underlined.

Keywords: acceleration of particles, sun: particle emission, sun: radio emission, sun: flares, sun: coronal mass ejections

1 INTRODUCTION

It has been shown in the companion chapter how radio observations can shed light on processes of impulsive particle acceleration and the propagation of charged particles in the corona and the Heliosphere. But it is clear that many SEP events are much longer than the duration of even the longest groups of type III bursts. Transport models deriving the injection function from electron observations also show that certain events need much longer episodes of particle release.

In their seminal review of early radio observations of the Sun Wild et al. (1963) proposed that two categories of particle accelerators were at work in solar eruptive events. On the one hand numerous flare-related events where non-thermal electrons are accelerated to up to 100 keV in the impulsive flare phase, as demonstrated by hard X-ray and microwave bursts, with direct access to open field lines toward the Heliosphere, as shown by type III bursts. The authors state - erroneously, as seen from today - that there was no evidence for energetic proton acceleration during this phase. On the other hand, in relationship with large flares from complex active regions, relatively rare, and presumably more energetic, events take place when metre-wave type II bursts show the presence of coronal shock waves, and type IV continua the presence of electrons in coronal magnetic structures well after the impulsive phase of the parent flare. Since the idea at that time was that type IV continua are produced by incoherent gyrosynchrotron emission, the radio continuum was taken as evidence of electron acceleration to MeV-energies. The authors noted that it is this category of events where large SEP intensities are observed in the Heliosphere. Wild and coworkers argued that different acceleration processes were needed to explain bursts of second-duration from electron beams in the impulsive flare phase and more smoothly evolving radio emission in the post-impulsive flare phase, and that Fermi acceleration at coronal shocks was the natural candidate in the post-impulsive phase. The later discovery of CMEs and their close association with radio bursts of types II and IV apparently substantiated this conclusion (e.g., Reames, 1999).

In this chapter the relationship of long-lasting SEP events with bursts of types II and IV is investigated. In **Section 2** the radio signatures of coronal shock waves associated with type II bursts are examined. The Mach numbers involved are discussed with respect to other observations in the corona and to data-driven models of CMEs. The statistical association between type II bursts and SEP events is then examined. In **Section 3** a more detailed investigation of two relativistic SEP events is presented, in order to study how the statistical associations manifest themselves in individual events. The Fermi/LAT telescope observed bursts and long-duration enhancements of gamma-rays produced by the decay of pions, which are themselves due to protons or He nuclei with a minimum energy of about 300 MeV/nucleon. These unique signatures of relativistic protons in the solar atmosphere are ideal counterparts of relativistic SEP events, but few relativistic SEP events could be compared with the gamma-ray observations so far. The gamma-ray observations are confronted with the type II and type IV radio emission in

Section 4. The chapter concludes with a short discussion of the role of radio observations in the future studies of SEP events from vantage points close to the Sun.

2 RADIO EVIDENCE OF SHOCK WAVES AND THEIR ROLE IN SEP ACCELERATION

2.1 Type II Radio Bursts

In a dynamic spectrogram type II bursts appear as one or several narrow bands of emission that gradually drift from high to low frequencies. Examples of such spectra are shown in **Figure 1** of the chapter by Vourlidis et al. In well-developed type II bursts two different bands can be distinguished, with frequency ratio of about 2, which are considered as emission at the plasma frequency (fundamental emission) and its harmonic. *In situ* measurements of electrons and waves at some interplanetary shocks driven by CMEs (Bale et al., 1999; Fitzenreiter et al., 2003; Pulupa and Bale, 2008) confirm the classical picture of type II emission that was inferred from radio observations at metre wavelengths and by analogy with the Earth's bow shock: electrons reflected at the shock form suprathermal beams in the upstream region, where Langmuir waves are also detected. The co-spatiality of reflected electrons with Langmuir waves is considered to be a consequence of wave amplification by the bump-on-tail instability. Deficiencies of the beams in the loss cone confirm their origin by reflection at the shock front. The shock geometry is reported to be quasi-perpendicular. This finding is consistent with the observation of energetic electrons at the Earth's bow shock (Burgess, 2007; Cairns, 2011) and with many models of type II burst emission in the corona (Holman and Pesses, 1983; Benz and Thejappa, 1988; Mann et al., 2018). This geometric requirement can explain why coronal radio sources are in general limited in space - a feature that is also suggested by the small (about 30%) relative bandwidth of the fundamental and harmonic bands of the type II burst (Mann et al., 1995).

The electrons generating the type II emission are themselves not very energetic: the measured distribution functions near 1 AU (Bale et al., 1999; Fitzenreiter et al., 2003; Pulupa and Bale, 2008) show beams at velocities of about 4,000 to 10,000 km s⁻¹ (energies 25–280 eV), although the observed electron spectra may extend to much higher energies. Using the drift rate of “herringbone” radio bursts excited by electron beams accelerated at type II shocks in the solar corona, Mann and Klassen (2005) estimated the typical energy of the beams as 7 keV, with a broad range up to 80 keV (see also Cairns and Robinson, 1987). The values depend on a coronal density model.

Shock waves giving rise to type II bursts are formed over a broad spatial range from the corona to the interplanetary space. Imaging observations localize high-frequency sources of type II emission (dm-m-wavelengths) within a fraction (~0.3) of a solar radius above the photosphere (Dauphin et al., 2006; Zimovets et al., 2012). The start heights of type II bursts at decametric wavelengths are inferred to lie at or above a solar radius above the photosphere (Gopalswamy et al., 2013; Shanmugaraju et al., 2017).

It is not clear whether the parent shocks have a unique origin, such as the shock wave driven by a fast CME. For long time it has been difficult to understand the relationship between metric type II bursts observed from ground and decametric-to-kilometric bursts observed from space, because of the gap created by the ionosphere between the two spectral domains. The Bruny Island Radio Spectrometer (BIRS) exploited the unique opportunity at its site to observe at frequencies down to 5–10 MHz, creating a seamless coverage of type II spectra from ground to space. In a systematic study Cane and Erickson (2005) distinguished different categories of type II bursts. The coronal type II bursts observed at metre wavelengths were found to have occasional extensions into the decametric range, but to be always limited to emission at heliocentric distances within $10 R_{\odot}$. Well-defined type II bursts from shocks in the interplanetary medium, on the other hand, were found to start higher in the corona, sometimes at frequencies that were clearly below those of a simultaneous metre-wave type II burst. The “interplanetary” type II bursts had diffuse broad bands of relatively faint emission, and were always associated with particularly fast CMEs. This was confirmed by the follow-up study of Pohjolainen et al. (2013), which showed that among 25 broadband type II bursts 24 were accompanied by CMEs with speeds between 1,200 and 2,600 km s⁻¹. These authors localized the radio source near the CME front in most cases (18/25), and behind the CME front in the remaining cases. This localization relies, however, on a model of the ambient electron density. Using direction-finding techniques from two spacecraft, Magdalenic et al. (2014) and Jebaraj et al. (2020) localized type II sources on the flanks of CMEs, and related them to interactions between the shock waves and streamers.

The most frequent category of low-frequency type II bursts identified by Cane and Erickson (2005) were spectral structures of narrow bandwidth and short duration that were aligned in the dynamic spectra along lines with drift speeds typical of interplanetary shocks. They were also identified in the (1–10) MHz range around the broadband events (Pohjolainen et al., 2013). This variety of features can be ascribed to different shock geometries, different emission processes (Bastian, 2007), and different drivers. Small-scale expanding loops in active regions (Klein et al., 1999b; Klassen et al., 2003; Su et al., 2015), shocks produced by the lateral expansion of CMEs (Stewart and Magun, 1980; Vainio and Khan, 2004; Pohjolainen et al., 2013), and blast waves (Claßen and Aurass, 2002; Vršnak and Cliver, 2008; Magdalenic et al., 2012) can create shorter-lived shocks than fast CMEs on their travel through the interplanetary space. Reiner et al. (2001) concluded that type II bursts in different wavelength ranges are different, finding that there was a correlation between the CME speed and the drift rate of type II bursts at DH wavelengths, which was confirmed by Pohjolainen et al. (2013), while no correlation was found at metre wavelengths. The absence of a correlation with the type II bursts at metre-wavelengths was confirmed by the detailed study of Mancuso (2007), which employed ground-based coronagraph and EUV observations in addition to SoHO/LASCO.

The overall spectral extent of the type II bursts is related to the energy of the associated CME: Gopalswamy et al. (2005)

conducted a systematic analysis distinguishing three types of type II bursts. They found the events to be ordered by increasing speed and width of the associated CME, both projected onto the plane of sky, from pure metre-wave type II bursts without DH counterpart over DH type II bursts with or without metre-wave counterpart to type II bursts extending from metric to kilometric wavelengths. The authors relate this ordering to the increasing kinetic energy of the CME. The interpretation translates a statistical relationship into a physical picture. But all statistical relationships show that a greater number of observable phenomena appears with the increase of the amount of energy released during an eruptive event - a phenomenon that Kahler (1982b) called the big flare syndrome. For example, the kinetic energy of CMEs is statistically related to the energy released to coronal heating, as measured by the soft X-ray fluence (see Figure 8 of Gopalswamy, 2009, and further references therein).

2.2 Mach Numbers of Shocks Associated With Type II Radio Bursts

A number of attempts have been undertaken to determine the Mach number of coronal shocks. Many of these estimates were based on type II bursts in the corona. They yield low values, between one and two for the Alfvénic or the fast magnetosonic Mach number (Smerd et al., 1975; Mann et al., 1995; Vršnak et al., 2002; Cho et al., 2007; Nindos et al., 2011; Zimovets et al., 2012; Mancuso and Garzelli, 2013; Kishore et al., 2016; Salas-Matamoros et al., 2016). The diagnostics rely on the hypothesis that the occasionally observed doubling of the drifting bands in the type II spectrum, called band splitting, shows simultaneous emissions from upstream and downstream of the shock front. The interpretation is disputed based on shock observations near 1 AU (Cairns, 2011) and on solar radio observations (Du et al., 2015), but has observational support from type II observations closer to the Sun (Vršnak et al., 2001; Mancuso and Garzelli, 2013). The method can only detect moderately strong shocks, because for high compression ratios the distinction between split bands of a given type II lane is blurred by the simultaneous presence of fundamental and harmonic lanes. For the 2002 Jul 23 CME, for which they derived a peak velocity above 2000 km s⁻¹, Mancuso and Avetta (2008) inferred an Alfvénic Mach number of 2.4 from the band splitting.

Comparisons of different methods using radio data and modeling in individual event studies show consistent results (Zucca et al., 2018; Maguire et al., 2020). The Mach numbers from the type II burst analyses are also similar to values derived from interpretations of many large-scale waves observed in EUV and soft X-rays (Warmuth et al., 2004; Muhr et al., 2011; Warmuth, 2015). Many coronal shocks, including type II shocks at metre wavelengths, are probably intrinsically weak (see also Mann et al., 1995). This is consistent with the idea that many metric type II bursts do not extend to lower frequencies because of a maximum of the Alfvén speed in the high corona, where the outward traveling shock decays (Warmuth and Mann, 2005, and references therein). The presence of a type II burst during a solar eruptive event, especially when it is restricted to

metre wavelengths, does not by itself reveal a strong shock and an efficient particle accelerator.

Considerably higher Mach numbers are reported for some CMEs based on coronagraphy and data-driven modeling of the shocks. Kwon and Vourlidas (2018) computed density compression ratios from coronagraphic observations in two CMEs, and derived Mach numbers using MHD Rankine-Hugoniot relations for a polytropic index 5/3. They inferred alfvénic Mach numbers up to 5. The basic uncertainty of this method comes from the line-of-sight integration of the coronagraphic images. Occasionally found compression ratios above four also question the assumed polytropic index. Rouillard et al. (2016), Kouloumvakos et al. (2019) and Kozarev et al. (2019) modeled the ambient coronal density and magnetic field, and inferred Mach numbers from stereoscopic observations and modeling of the erupting structures. They derived fast magnetosonic Mach numbers as high as 10. The advantage of this method is that it can identify local peculiarities of the Mach number, such as enhancements near magnetic neutral lines, which are smeared-out by the spatial integration in the coronagraphic density measurements. The high Mach numbers, which are calculated from the modeled Alfvén speed, cannot be checked by any method relying on the measurement of compression ratios, such as the analysis of type II split bands, since for high Mach numbers the relationship with the density compression ratio depends critically on the basically unknown polytropic index.

2.3 Type II Bursts and SEP Events

2.3.1 Statistical Associations

Early attempts to relate SEP events to metre-wave type II bursts on statistical grounds failed, since metre-wave type II bursts were found to be accompanied by type IV bursts, and on occasion type IV bursts without clear type II emission at metre wavelengths were found to be associated with SEP events (Kahler, 1982a). The search for statistical associations intensified again when systematic observations of radio emission at decametric to kilometric wavelengths from space became available in the late 1970s. Since type II bursts at decametric and longer wavelengths are typically generated at heliocentric distances above $2 R_{\odot}$, they allow for a direct comparison with the propagation of CMEs observed by space-borne coronagraphs.

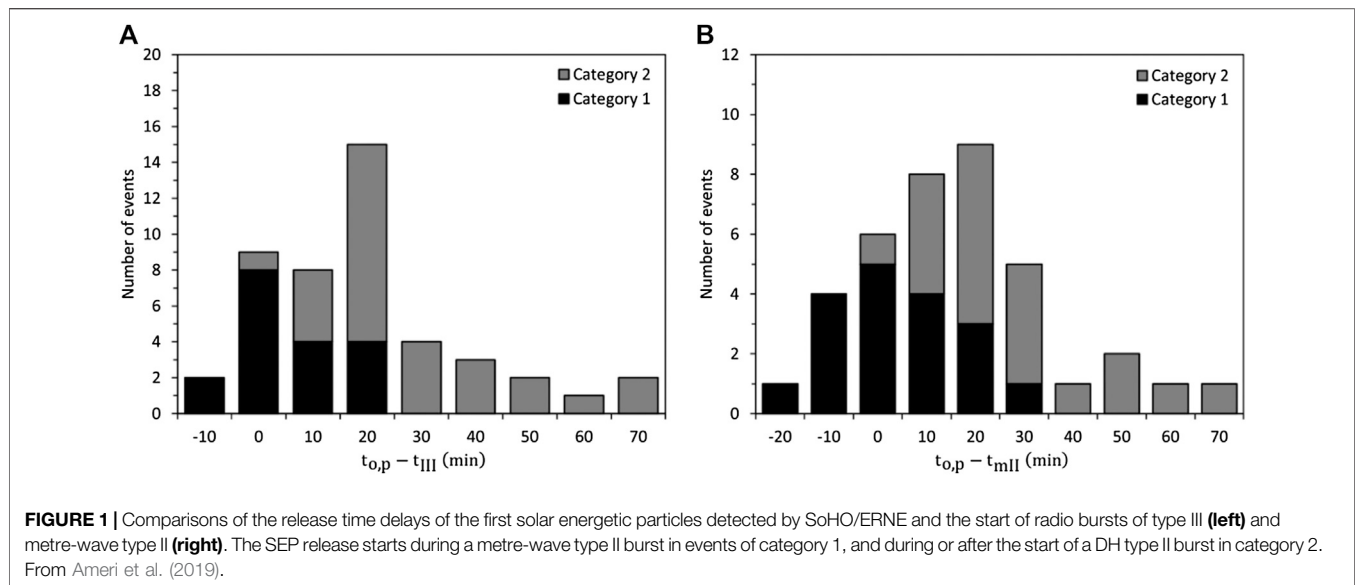
Cane and Stone (1984) showed that most type II bursts at frequencies below 2 MHz (32/37) were accompanied by SEPs at energies above 18 MeV/nuc. Gopalswamy et al. (2002) confirmed this result with Wind/WAVES observations (frequencies <14 MHz) for SEP events with fluxes above 10 pfu ($1 \text{ pfu} = 1 \text{ cm}^{-2} \text{ s}^{-1} \text{ sr}^{-1}$) at energies above 10 MeV (40/42 events), and a weaker association for weaker SEPs. In line with the above studies Cliver et al. (2004) found that while less than half of the metre-wave type II bursts observed 1996–2001 with eruptive activity in the western solar hemisphere were associated with SEPs of energy >20 MeV, the association increases to 90% for type II bursts that extended into the range (1–14) MHz.

The above work considered radio events, and looked at the correlation with SEPs. Cliver et al. (2004) also made the inverse approach, considering a sample of 88 SEP events above a peak-intensity threshold of $10^{-3} \text{ cm}^{-2} \text{ s}^{-1} \text{ sr}^{-1} \text{ MeV}^{-1}$ at energies above 20 MeV. They found 91% of the events accompanied by a type II

burst, be it at metre wavelengths, deka-to-hectometre wavelengths, or both. The association of SEP events with both types of type II bursts was found to increase with the SEP peak intensity. The few SEP events that had no type II emission associated were weak. Similar results were found in other studies (Gopalswamy et al., 2005; Richardson et al., 2014; Kouloumvakos et al., 2015; Ameri et al., 2019). The rate of association of SEP events above 25 MeV with DH type II bursts quoted by Richardson et al. (2014) is only 47%. This could be due to a relatively larger fraction of weaker events in that study as compared to Cliver et al. (2004).

Gopalswamy and coworkers (Gopalswamy et al., 2008a; Gopalswamy et al., 2008b) went one step further and distinguished the SEP association of fast CMEs with and without type II bursts. They compiled two samples of fast (projected speed of at least 900 km s^{-1}) and wide (width $\geq 60^\circ$) CMEs, and distinguished those that were accompanied by a type II burst at metre-wave or DH wavelengths (“radio-loud”; 268 cases) from those which were not (“radio-quiet”; 193 cases). The authors showed that none of the radio-quiet CMEs was accompanied by an SEP event satisfying the NOAA criterion that the proton flux exceed 10 pfu at energies above 10 MeV. Only 13/193 were accompanied by minor enhancements of the SEP intensity. Again there is some effect due to the intrinsic size of the events that can be related to the big flare syndrome: the radio-quiet CMEs are on average slower and narrower than the radio-loud ones, and also the SXR burst importance is lower for radio-quiet CMEs (C6.9) than for radio-loud ones (M3.9). In addition the parent eruptive activities of the two CME-samples have different locations: 211/268 (79%) radio-loud CMEs have their parent activity on the disk, but only 81/193 (42%) of the radio-quiet ones. So one may have to worry about the visibility of type II emission or SEPs in some of the radio-quiet CMEs. The type II signature appears here as a necessary ingredient to show that a CME drives a shock wave. In the interpretation of Gopalswamy et al. (2008b) the radio-quiet CMEs are those which propagate through coronal regions with high Alfvén speed and therefore do not drive powerful shocks, despite their high speed. The absence of significant SEP events with the radio-quiet CMEs is interpreted as a new piece of evidence that the SEPs are accelerated at the CME-driven shock wave. While the statistical studies based on type II emission leave some ambiguity, the suggested close connection between SEP acceleration and CME-related shocks is confirmed by the combination of CME observations and modeling of the corona, which shows a correlation between SEP peak intensities in the energy range (20–100) MeV and the shock Mach numbers (Kouloumvakos et al., 2019).

Iwai et al. (2020) studied CMEs from the western solar hemisphere with a rather narrow range of speeds ($1,200\text{--}1,800 \text{ km s}^{-1}$) and discovered a correlation between the peak SEP flux at energies above 10 MeV and the spectral width of the type II burst at hectometre wavelengths. They interpret the bandwidth as an indicator of the capacity of electron acceleration of the shock, and consider the correlation as additional evidence that CME-driven shocks that are efficient electron accelerators are also efficient accelerators of SEPs. Cliver and Ling (2009) examined how the finding that large SEP events are associated with type II bursts and vice versa fits into the scenario (e.g.,



Reames, 1999) that the numerous small “impulsive” SEP events are particles escaping from the flare site, while the rare large “gradual” SEP events are accelerated by CME-driven shocks. They found that only 5% of the impulsive SEP events are associated with DH type II bursts, but 95% of the gradual events.

2.3.2 The Relative Timing of Initial SEP Release and Type II Bursts

A more detailed comparison of the timing of shock signatures and the onset of SEP events became possible with the high energy resolution of the Wind/EPACT and SoHO/ERNE instruments. Reames (2009), Kouloumvakos et al. (2015) and Ameri et al. (2019) analyzed the times of first SEP detection at the spacecraft as a function of particle energy, and inferred the solar release time from a velocity dispersion analysis (cf. Section 3.1.1 of the companion chapter). The detailed analyses by Kouloumvakos et al. (2015) and Ameri et al. (2019) confirm that velocity dispersion analysis is far from straightforward, since discrepancies between the initial solar release times and the interplanetary path lengths inferred in the two studies may exceed by far the quoted statistical uncertainties.

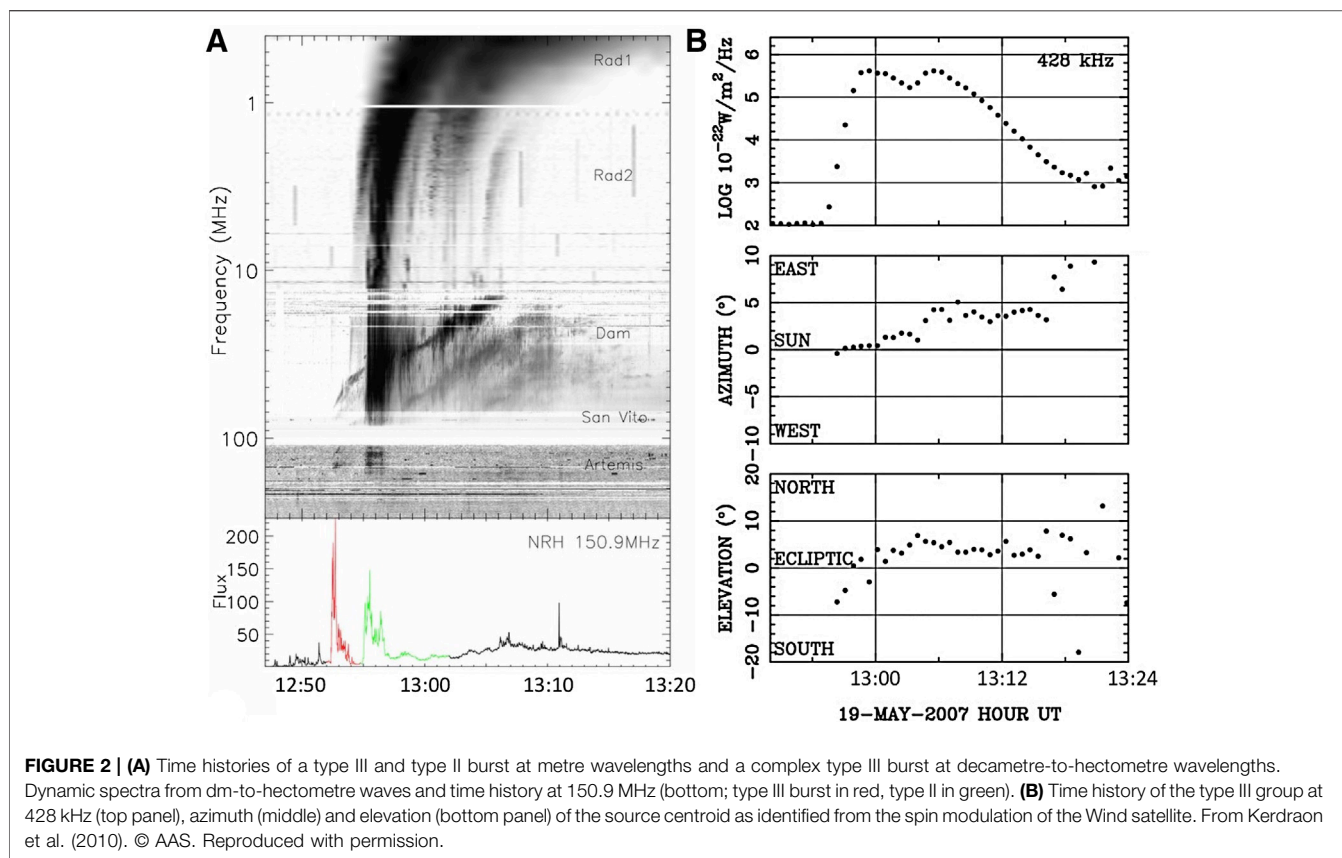
The differences between the release of the first energetic protons and the start of the type III and the metre-wave type II emission is shown by the two histograms in **Figure 1**. From the mere timing of the initial solar particle release it appears difficult to relate SEP acceleration preferentially to one of the two burst types. But Kouloumvakos et al. (2015) report that in many cases where type II and type III bursts were present, the type III bursts emanated from the type II bursts, which suggests that the electron beams emitting the type III bursts actually were accelerated at the coronal shock waves, as originally suggested by Cane et al. (1981) and Dulk et al. (2000). This interpretation will be further discussed in **Section 2.4**.

Kouloumvakos et al. (2015) conclude from their timing analysis that 28% of the SEP events are consistent with an initial release before the type II burst, but that these events tend to have softer (steeper

spectra than those where the initial release occurs during a type II burst. Ameri et al. (2019) conclude that the initial SEP release is always accompanied by a metric or DH type II burst, and that the energy spectra tend to be harder when the initial release occurs early, which means at the time of a metre-wave type II burst or before the start of a DH type II burst (events in their category 1). Under the hypothesis that the association with type II emission reveals acceleration at the CME shock, they derive that the SEP acceleration starts when the nose of the shock is at heliocentric distances between 2.0 and 3.5 R_{\odot} (Kouloumvakos et al., 2015), while Ameri et al. (2019) find a much broader distribution between 1 and 4 R_{\odot} for the events starting before the DH II burst, and 1–9 R_{\odot} for those that start during the DH II burst.

Reames (2009) included relativistic solar particles from neutron monitor observations in his velocity analysis and found that the initial proton release was always delayed with respect to the start of the metric type II burst, the delays varying between about 4 and 38 min. He concluded that the initial release of energetic particles from energies ranging from 1 MeV to 1 GeV and more was simultaneous, and was due to the acceleration at the shock, which radio observations showed to exist at that time. The inferred heliocentric distance where the particle acceleration started was in the range (2.4–5.7) R_{\odot} . The delayed release with respect to the appearance of the type II burst can be explained by an initial shock formation in regions of closed magnetic fields in the low corona, so that the first accelerated particles remain trapped. This is what Rouillard et al. (2016) find during the 2012 May 17 event. They report from their detailed observations combined with modeling of the CME observations and the ambient corona that the SEP release starts when the shock and in particular the regions of high Mach number proceed to open magnetic fields.

These statistical associations demonstrate that type II bursts are a common element of an eruptive event that produces high SEP fluxes. Only SEP events with weak proton fluxes occur without a recognisable type II burst. In the light of the conclusion by Kahler (1982a) it is interesting to examine whether the association with type



II bursts is exclusive as to the radio counterpart of SEP events. Cane and Stone (1984) list the association of their events with radio bursts of both type II and type IV. Metre-wave type IV bursts accompanied 30/37 DH type II bursts. Four of the DH type II bursts were not accompanied by SEPs. It may be relevant that three of these had no type IV burst associated either, and that in the fourth event without SEPs the type IV burst is noted as “possible”. Three further DH II bursts with SEP events had no type IV counterpart. This looks like a comparable rate of association of SEPs with DH type II bursts and metric type IV bursts, rather than a preferential association with type II bursts. Both Kouloumvakos et al. (2015) and Ameri et al. (2019) argue that type II bursts are more closely related with their SEP events than type IV bursts. Closer inspection of their events where presumably no type IV emission was found shows, however, that a number of them occurred behind the limb, where type IV emission might be occulted, while in others type IV bursts seen in single-frequency records or radioheliographic observations apparently left no trace in the dynamic spectra examined by these authors. It looks like the correlation between SEP events and type II bursts, however important it is, may by itself not be a statistical proof that the CME shock is the only or even the dominant particle accelerator.

2.4 Complex Type III Bursts, Type II Bursts, and Particle Acceleration After the Impulsive Flare Phase

Complex type III bursts were introduced in the companion chapter. They actually show a similarly ambiguous relationship

with type II bursts as SEP events. The idea that these bursts are just longer versions of classical type III bursts associated with the impulsive flare phase was contradicted by Kundu et al. (1990), who discovered that they may come from different locations. This was confirmed by Kerdraon et al. (2010) and Jebaraj et al. (2020). **Figure 2A** displays the time history of a complex type III group (two top panels) and radio emissions at higher frequencies. The group of hectometric type III bursts starts with the impulsive metre-wave type III emission, but lasts much longer. It is accompanied by type II and type IV bursts at metre wavelengths. But the distinction between the early and late phase of the type III group is not only one of timing. The direction finding technique shows (**Figure 2B**) that the positions of the type III bursts in the impulsive flare phase differed from those in the post-impulsive phase. Reiner et al. (2008) showed that late complex DH type III bursts were also associated with different sources and different types of dm-m wave emission than the preceding DH III bursts in the impulsive phase of the parent flare.

The different position of the impulsive and post-impulsive type III sources means that the acceleration region and the magnetic connection to the Heliosphere changed. A common interpretation suggested by the observation of a metric type II burst (**Figure 2A**) is that the post-impulsive electron beams are accelerated by the shock wave. From their direction finding analysis Jebaraj et al. (2020) found indeed that the type III bursts in the impulsive phase and those in the post-impulsive phase were located on either side of a CME, and that the late type

III bursts were on the same side as the type II source. The shock origin of complex DH type III groups has long been favored (Cane et al., 1981; Dulk et al., 2000). Klassen et al. (2002) studied an event (1998 May 19) where the only radio counterpart of the eruption of a large quiescent filament was a type II burst with type III bursts emanating from the type II spectrum, and no emission at higher radio frequencies. The close relationship with the type II burst and the absence of radiative signatures from an alternative origin point toward shock acceleration of the electron beams. This is, however, an exceptionally pure case, which was associated with a small electron event that extended to relativistic energies (> 250 keV), and a faint proton event at MeV energies observed by SoHO/EPHIN and ERNE. Cane et al. (2002) observed that the long-duration DH type III bursts accompanying SEP events at energies above 20 MeV start on occasion at frequencies above the type II burst, may last longer than the type II burst, and could even occur without a type II burst (see their Figure 5). Type IV continua at lower altitudes than the shock were shown by a number of investigations to be a typical counterpart of long-lasting DH type III burst groups (Klein and Trotter, 1994; Reiner et al., 2000). On occasion, such broadband emissions, including the DH III bursts, show correlated variations across the entire frequency range, which may include hard X-rays from the chromosphere (Trotter, 1986; Pick et al., 2005; Reiner et al., 2007). In other events the spectra show gyrosynchrotron emission from centimetric to metric wavelengths (Dauphin et al., 2005; Vršnak et al., 2005; Carley et al., 2017). Correlated variations of these emissions, which are produced by non-thermal electrons with different lifetimes in different environments of the solar atmosphere, can only be understood by a modulation of a time-extended process of electron acceleration in the corona (Cliver et al., 1986; Trotter, 1986). This does not exclude shock waves, but an accelerator that resides in the corona downstream of the outward propagating CME appears as a more natural accelerator over tens of minutes or even longer durations. Cliver et al. (1986) proposed to relate the electron acceleration in type IV bursts to magnetic reconnection in the wake of the CME.

An alternative acceleration scenario is related to CME propagation through the low corona. The sequence of type III bursts in **Figure 2** occurred with a weak eruptive flare (GOES class B 9.5), accompanied by an EUV wave, near solar minimum in 2007. Groups of type III bursts showed the typical sequence with a first packet that started at metre wavelengths (250 MHz) and a second starting at lower frequencies (near 20 MHz), hence probably higher in the corona. At 150 MHz type III sources in the first group are observed to occur at gradually increasing distance from the parent active region. Their westward displacement follows the propagation of the EUV wave. The direction-finding observations from Wind/WAVES at 428 kHz show sources at different positions during the first and second group of type III bursts. Like for the metre-wave bursts, Kerdraon and coworkers relate the displacement of the interplanetary radio sources at a heliocentric distance of 0.15 AU to the expansion of the EUV wave in the low corona. The type III bursts were accompanied by a type II burst at metre-wavelengths. The source of its harmonic emission was close to that of the metre-wave type III bursts. The authors interpret the radio signatures as the

consequence of electron acceleration at the interface between the expanding CME, traced by the EUV wave, and the ambient corona. In a similar case analyzed by Salas-Matamoros et al. (2016) a smaller group of type III bursts and a type II burst were found late during a flare, at a time when the CME had reached remote open magnetic field lines. The type III bursts were accompanied by a type II burst, but started at higher frequencies. While shock acceleration is not excluded, the starting frequency of the type III bursts is better explained by electron acceleration in relationship with magnetic reconnection between the CME and the surrounding corona.

Radio emissions therefore show a variety of phenomena that point to different acceleration processes after the impulsive flare phase. They are clearly related to CMEs, either by the reconnection they trigger in their aftermath or by their interaction with the ambient corona. The very simple solar minimum events analyzed by Klassen et al. (2002), Kerdraon et al. (2010), and Salas-Matamoros et al. (2016) support different acceleration processes, which may act during the same event and release energetic particles into different regions of the heliosphere. The complexity of this situation cannot be entirely captured by statistical analyses.

2.5 Coronal Mass Ejections, Shocks, Type II Bursts, and SEP Acceleration - A Summary

The long durations of the large “gradual” SEP events observed at energies up to tens, possibly hundreds of MeV in space and their association with fast CMEs are a strong argument that the shock wave driven by the CME is an efficient particle accelerator. The type II radio emission is an important diagnostic, which shows especially that there is no unique category of “fast” CMEs, but that the ability to drive a shock wave depends on the ambient medium. The preferential association of SEP events with CMEs accompanied by a type II burst reinforces the idea that the shock wave is necessary for the SEP production. Sophisticated modeling shows the correlation between high Mach numbers, which are especially found in the vicinity of current sheets, and high SEP intensities at tens of MeV.

The radio emissions are a hint that acceleration processes of different nature operate in the corona: the type III bursts typical of the impulsive flare phase, which on occasion also operate later in the solar eruptive event, reveal repetitive short and fragmented acceleration processes. Their absence during much of the late acceleration phases observed in the corona through the type IV radio emission and its occasional hard X-ray counterpart, and during the time-extended electron acceleration revealed by transport modeling, suggests that at least the acceleration of the radio-emitting and the near-relativistic electrons is smoother and likely due to different acceleration regions and different acceleration processes. The scenario devised by Wild et al. (1963) and adopted for SEP acceleration by Reames (1999), which attributes the sole or dominant role of particle acceleration in large SEP events to coronal shock waves, is very popular. The popularity may, however, draw more justification from the intrinsic simplicity of the scenario than from the observations.

Type II bursts seem indeed to be often produced by rather weak shocks, which are not expected to accelerate protons and

ions. The statistical studies also show a general trend that the manifestations of type II bursts become more frequent and more varied as the energy of the parent eruptive event, especially of the CME, increases. Under these conditions statistical correlations may be spurious. This recalls the interdependence of parameters related to the flare emission and the CME characteristics mentioned in the companion chapter. This interdependence is also found in the statistical relationships between SEP intensities and the parameters of the related radio bursts of type III and type II: In the attempt to devise a radio index able to serve as a forecasting tool of SEP events, Winter and Ledbetter (2015) conducted a principal-component analysis using parameters of DH II and DH III bursts associated with SEP events. The most promising index in the light of their study takes into account properties of both types of radio emission, namely the flux density and duration of type III bursts, and the peak flux density and fluence of type II bursts. This result is another indication that considerations of statistical association do not single out type II bursts as a key radio activity related to large SEP events.

Radio observations of type II bursts have some unexploited potential for improving diagnostics of coronal shock waves. Spectral imaging is now possible with instruments such as the Low-Frequency Array (LOFAR) and the Murchison Widefield Array (MWA), while in earlier times one could only image spectral features of type II emission at single frequencies. The new capacities should allow further investigation on the interpretation of split bands, which is controversial, because no hint on radio emission downstream of a shock wave is found in in situ observations near 1 AU. Observations with Parker Solar Probe and Solar Orbiter should show us whether the objections at 1 AU are valid close to the Sun. Spectral radio imaging should also allow us to more precisely investigate the frequency drift of type II bursts and its relationship to the shock speed. Traditional methods use spherically-symmetric density models, but the radio source is likely located in the quasi-perpendicular region of the shock, which may be on the flank of the CME, and which may change place with respect to the shock front as the CME progresses through the corona.

A major problem of statistical studies is the possible exclusion of relevant information, for instance in statistical correlations that favor type II bursts while disregarding type IV bursts. Shock waves are generated in the solar corona in relationship with processes that are themselves related to particle acceleration, such as magnetic reconnection in the wake of the CME. Case studies of SEP events and their relationship with electromagnetic emission in the corona may provide further indications toward relationships. In the next section relativistic solar proton events will be addressed, where the energetic particles detected in space or on the Earth have some time structure that can be compared with particle acceleration signatures at the Sun.

3 RADIO EMISSION AND RELATIVISTIC SOLAR PROTONS

SEP events can on occasion extend to relativistic energies, with values as high as a few tens of GeV reported in the literature for

extreme cases. While some spacecraft measure SEPs up to several hundreds of MeV (IMP-8, e.g. Tylka and Dietrich 2009; GOES/HEPAD, see Bruno 2017, and references therein; SoHO/EPHIN, Köhl et al., 2017) or even several GeV (PAMELA, Bruno et al., 2018), the traditional measurements with neutron monitors provide the largest data collection. Neutron monitors measure secondary particles produced by an atmospheric cascade triggered by a primary nucleon (Bütikofer, 2018), provided the primary has a minimum energy of about 450 MeV. An SEP event producing a detectable signal on ground is called a Ground-Level Enhancement (GLE). 72 GLEs were observed since 1942, initially by ionization chambers, and since the international geophysical year, with neutron monitors that now form a worldwide network.

SEP time profiles at Earth are heavily affected by propagation in the turbulent interplanetary magnetic field. The time profiles of particle intensity, for instance, carry few exploitable traces of the acceleration process. The most obvious criterion to compare with electromagnetic signatures of particle acceleration in the corona is the onset time. McCracken et al. (2008) and Moraal and McCracken (2012) showed that GLEs present a distinct time structure, which these authors relate to the magnetic connection between the Earth and the parent eruptive activity. In some cases the GLE starts with an impulsive peak seen only by neutron monitors sensitive to particles that reach Earth along the interplanetary magnetic field. The onset occurs close in time to the start of the flare. In the majority of GLEs, where the parent activity is far from the footpoint of the Earth-connected interplanetary magnetic field line, most neutron monitors see only a later, nearly isotropic distribution of primary particles, with some delayed onset. A primary example of the first, prompt GLE category, occurred on 2005 Jan 20 (McCracken et al., 2008). The time profiles of neutron monitors showing the early and the late component are plotted in the left panel of **Figure 3**. A major isotropic event occurred on 1989 Sep 29 (Moraal and Caballero-Lopez, 2014). A different account of the two event categories, based on the energy spectrum, was given by Vashenyuk et al. (2006). The classification is further discussed in Miroshnichenko (2001).

3.1 The Relative Timing of Radio Emission and the Onset of Ground-Level Enhancements

The GLE on 2005 Jan 20 (GLE 69) was associated with an eruptive flare located at W 58°. It was hence nearly ideally connected to Earth, and a privileged event for the comparison with electromagnetic signatures of particle acceleration in the solar atmosphere. The eruptive activity comprises a strong flare, large-scale EUV waves and a fast CME, analyzed in detail by Grechnev et al. (2008). The initial anisotropic component of the GLE (before 7:00 UT, **Figure 3A**) was closely connected in time with hard X-ray and microwave emission of energetic electrons, and pion-decay gamma-ray emission above 60 MeV from protons and α particles at energies above 300 MeV/nucleon (Grechnev et al., 2008; Masson et al., 2009). The time histories of the microwave, hard X-ray and gamma-ray emissions in **Figure 3B** show a time-structured impulsive phase with 1 min duration

episodes of acceleration indicated by the different levels of gray shading. The acceleration efficiency increases from episode 1 to 2: hard X-ray count rates and microwaves rise together in phase 1. The gamma-ray continuum above 60 MeV (see also Kuznetsov et al., 2008) stays at background at that time. It starts to rise in episode 2, where the hard X-ray spectrum is harder than in phase 1, and where the microwave flux density peaks. The gamma-ray spectrum shows the characteristic shape of pion-decay emission. The authors conclude that the gamma-ray time profile reveals the acceleration of protons above 300 MeV. In the decay phase the gamma-ray detectors show a constant level, which is likely produced by the impact of energetic protons. The impulsive phase acceleration hence shows a complex time structure, rather than a well-defined process that can be described by a delta-function. The time interval of intense microwave and gamma-ray emission in **Figure 3** is preceded and accompanied by radio emission that gradually drifts from high to low frequencies (Bouratzis et al., 2010). This shows the gradual extension of the coronal region to which energetic electrons are released, as discussed in *Section 4.1* of the companion chapter.

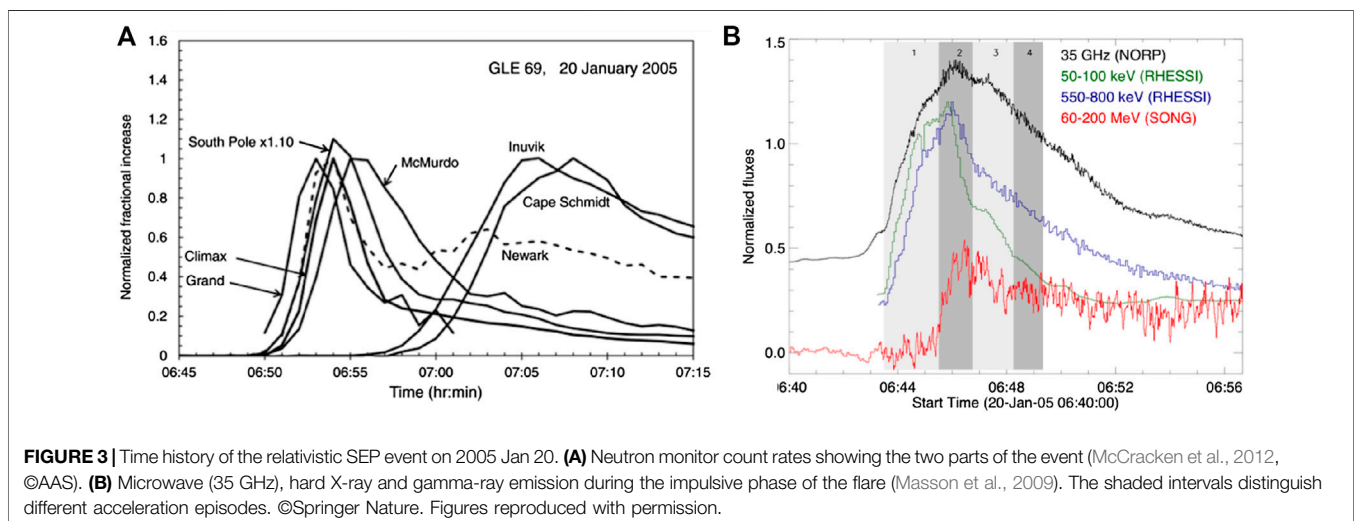
Type III bursts from decametric-to-kilometric wavelengths demonstrate that electrons escaped from the eruptive active region along open field lines since the acceleration episode 1. Hence relativistic protons, which were seen to be accelerated in close relationship with the electrons, were also able to escape. They are prime candidates to explain the early anisotropic phase of the GLE. The onset of the gamma-ray burst (06:45:30) and of the GLE (06:50, McCracken et al., 2008) imply an interplanetary path length of about 1.5 AU. This estimate suggests that the first relativistic protons at Earth were accelerated during the impulsive phase of the flare. McCracken et al. (2008) reached the same conclusion. They evaluated a larger delay between the onsets of the gamma-rays and the GLE. This is probably because they used smoothed gamma-ray count rates, where the smoothing process artificially advanced the steep rise.

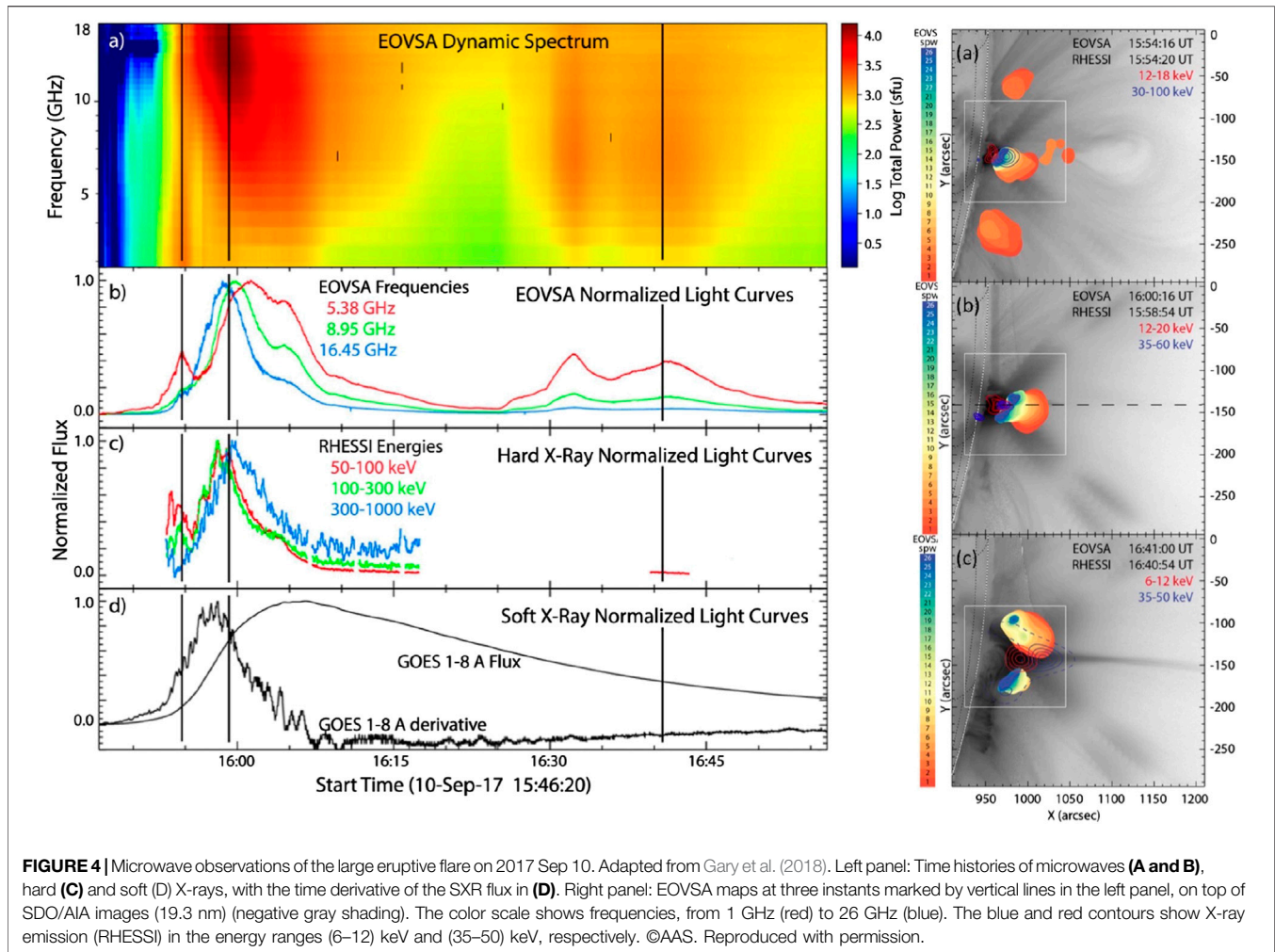
Reames (2009) concluded differently, attributing the relativistic SEP acceleration to the shock wave revealed by the

metric type II burst. He located the onset of the type II burst at 06:35.7 solar release time based on the photon arrival time at Earth (06:44.0 UT) reported by NOAA/SWPC (see also Figure 12 of Pohjolainen et al., 2007). At this time hard X-rays and microwaves show the presence of mildly relativistic electrons in the corona, but the strong pion-decay gamma radiation starts a minute later. The consistency between the onset of the gamma-rays, the start of the GLE, and the DH type III bursts which show the existence of open field lines from the flaring active region to the Heliosphere, are in favor of a close link between the acceleration of relativistic electrons and protons in the flaring active region, rather than the CME shock.

A second proton release started a few minutes later. This was the onset of the second part of the GLE as seen by the neutron monitors at Cape Schmidt and Inuvik in **Figure 3A**. It was associated with a new rise of the radio emission, with continuum emission (type IV burst) between a few GHz and tens of MHz. On its low-frequency side DH type III bursts showed again that open field lines were connected to the particle acceleration regions, which allowed electrons, and therefore also protons, to escape into the Heliosphere (Klein et al., 2014; Klein et al., 2015). No gamma-ray observations were available at that time. So the second part of the GLE showed again a close timing relationship with particle acceleration in the corona.

The GLE on 1989 Sep 29 (GLE 42) is different in that the anisotropic early peak was not seen, probably due to poorer magnetic connection of the Earth to the parent eruptive activity, which was slightly behind the western solar limb (Moraal and Caballero-Lopez, 2014). Klein et al. (1999a) compared the GLE onset with radio observations and showed that the first arrival of relativistic protons at Earth was better connected in time with a late type IV burst continuum that extended from centimetric to metric wavelengths, rather than with the impulsive phase emissions. The conclusion was reached earlier by Akimov et al. (1996) using transport modeling to relate the GLE on 1991 Jun 15, which lacked the initial anisotropic peak





(McCracken et al., 2012), to the associated microwave burst at 3 GHz. Akimov et al. (1996) showed that the GLE time profile was better fit by a model where the impulsive part of the microwave emission (at 3 GHz) was omitted.

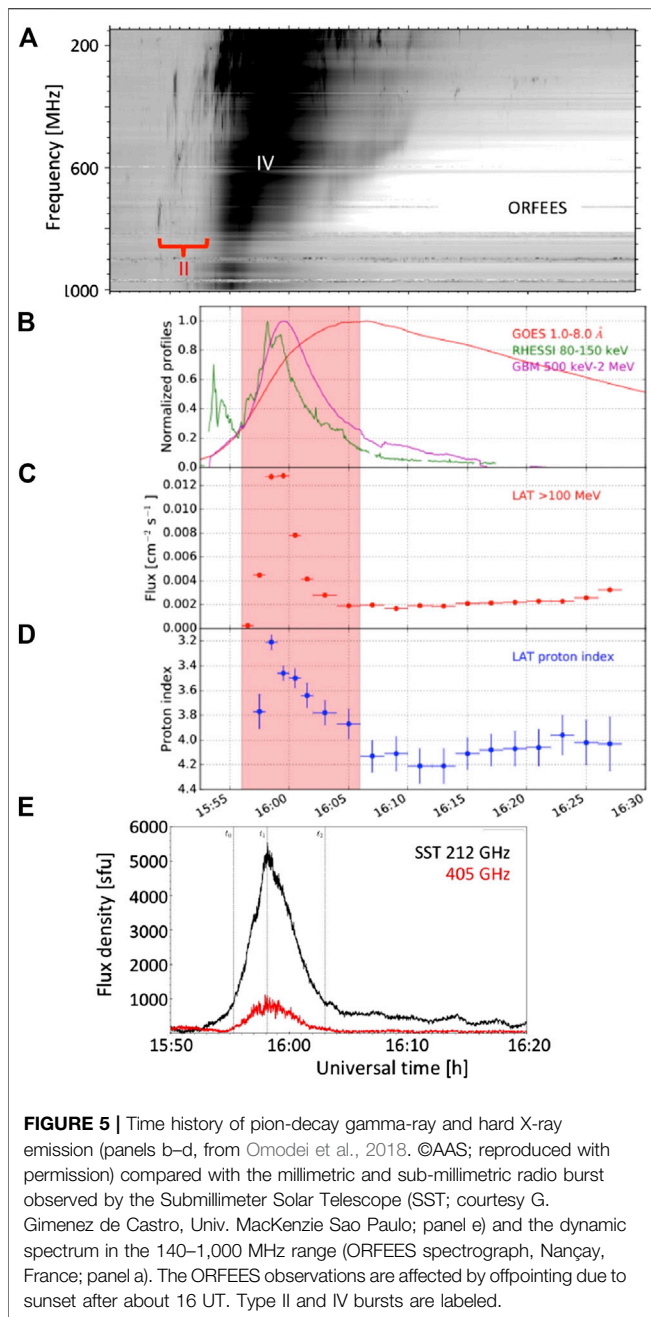
Moraal and Caballero-Lopez (2014) and Klein et al. (1999a) hence come to the same conclusion of two distinct solar releases during the prompt and the delayed phase. As in the case of 2005 Jan 20, the delayed particle release was related with distinct particle acceleration in the solar corona revealed by a type IV continuum. This does not exclude acceleration at the CME shock, at times when the CME is a few solar radii above the photosphere (Kahler, 1994; Reames, 2009; Gopalswamy et al., 2012). The delay is then attributed to the time needed for the shock to form and to reach open magnetic fields, and the time the shock needs to accelerate protons to GeV-energies. Numerical simulations by Afanasiev et al. (2018) show indeed that the acceleration needs about 10 min. In this case the timing relationship between the start of a delayed GLE and post-impulsive radio and hard X-ray signatures would have to be considered as fortuitous. However, the 2005 Jan 20 event shows that protons must be accelerated on shorter time scales. This makes it plausible that the timing of the delayed GLEs is indeed related to late acceleration, and the

relationship with the type IV emission argues for particle acceleration in the wake of the CME.

3.2 The GLE and Gamma-Ray Event on 2017 Sep 10

A major eruptive event (GOES class X8.2) at the solar limb produced a GLE (GLE 72) of modest intensity on 2017 Sep 10. The eruptive activity was observed with much detail in EUV and coronagraphic imaging, in microwaves, hard X-ray and nuclear gamma-ray emissions. Of particular interest are the good coverage of pion-decay gamma-rays by Fermi/LAT (Omodei et al., 2018) and the first microwave imaging observations with the Extended Owens Valley Solar Array (EOVSA; Gary et al., 2018).

EUV images, displayed as the gray-scale background images in the right panel of **Figure 4**, reveal a geometry close to the standard (CSHKP; see Janvier et al., 2015, for a recent review) solar flare scenario, with a rapidly outward-accelerating bulb-like feature (the light-gray - i.e., faint - bulb-shaped structure in Fig. a), interpreted as the rising flux rope, the sustained formation of an arcade of flare loops underneath, and a very narrow bright plasma



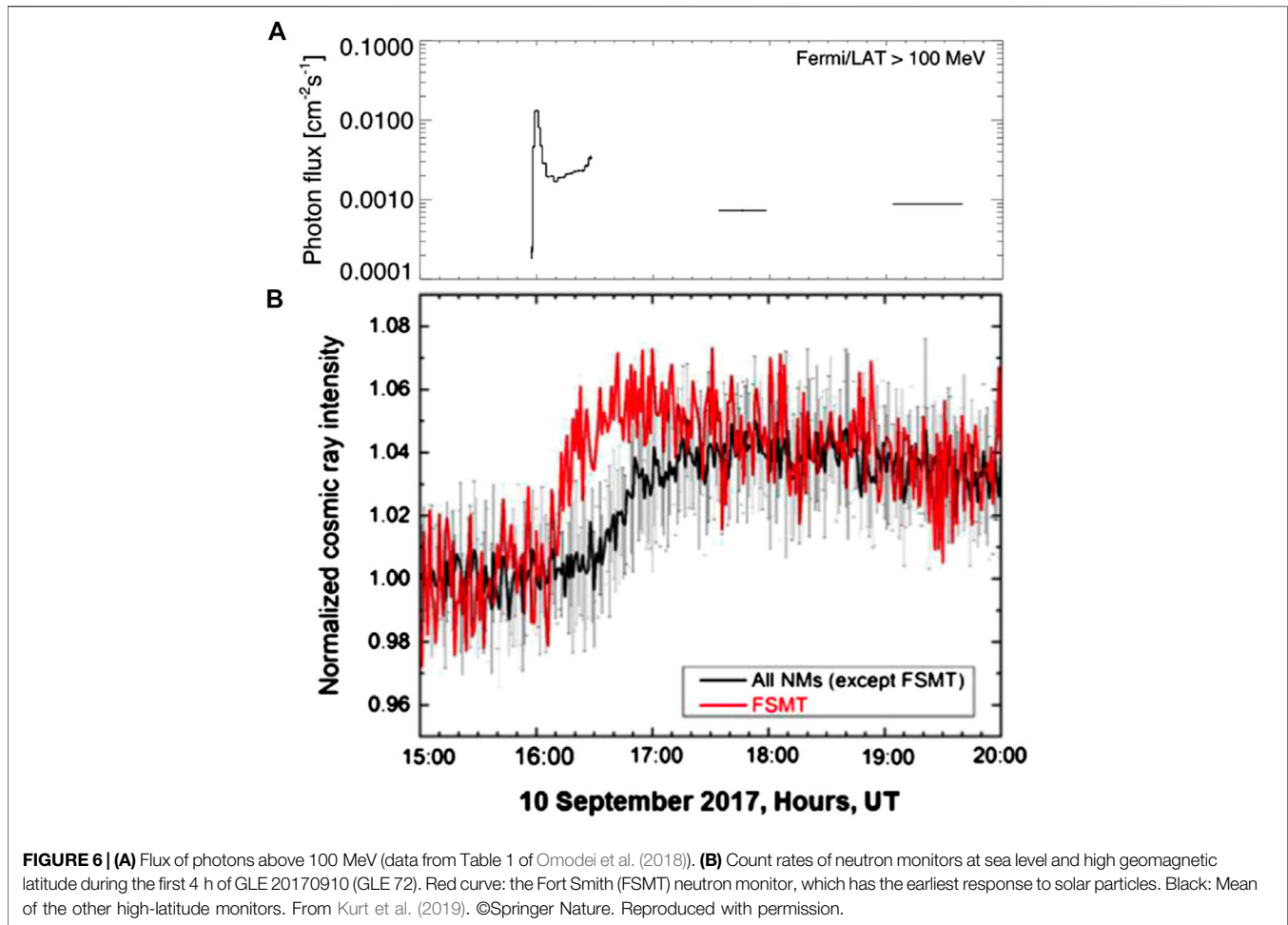
sheet that connects the top of the flare loops to the flux rope (Seaton and Darnel, 2018; Yan et al., 2018), visible as a dark narrow ray extending to the right border of the image in (c). Numerous studies of this plasma sheet show its dynamics and motions that are interpreted as plasma motions in and around a reconnecting current sheet (e.g. Warren et al., 2018).

The left panel of **Figure 4** displays the time histories in soft X-rays (d), hard X-rays (c), and microwaves (b), and a dynamic spectrum between 1 and 18 GHz (a). Gary et al. (2018) show that the impulsive phase ($\sim 15:50$ – $16:06$) actually consists of a series of “elementary” bursts with a trend toward a hardening electron spectrum, which is shown in the Figure by the increasing delay of

the hard X-ray time histories at higher energies. This is the same evolution as on 2005 Jan 20 (**Section 3.1, Figure 3B**). The maps of the microwave sources at the three instants marked by vertical lines in the left panel of **Figure 4** are shown in the right panel in colored shades on top of the EUV images. The dominant microwave source is located above the rising loop arcade, at the base of the plasma sheet. This location strongly suggests that the electrons are accelerated in the reconnecting current sheets embedded within the plasma sheet or by turbulence in the outflow region (see also Cai et al., 2019).

The time profiles of the gamma-ray and hard X-ray emission are shown in more detail in **Figures 5B,C**, combined with the time profiles at sub-millimetre wavelengths in panel E and the dynamic radio spectrogramme between 140 and 1,000 MHz in panel A. The sub-mm emission has a spectrum that decreases with increasing frequency, which points to gyrosynchrotron emission from relativistic electrons. At frequencies below 1 GHz a type IV burst is seen at that time (panel A), which is the continuation of the first burst seen by EOVS. The type IV burst is preceded by a type II burst that starts several minutes earlier at unusually high frequencies, near 800 MHz, during the early rise of the flux rope as displayed in Figure 2 of Seaton and Darnel (2018). The bright emissions at sub-millimetric and gamma-ray wavelengths accompany the type IV burst. The localization of the gamma-ray source by Fermi/LAT is consistent with the active region (Omodei et al., 2018). These observations strongly suggest that during the impulsive phase non-thermal to relativistic electrons and relativistic protons were accelerated together in the main region of energy release in the flare. The acceleration operated at about the same time on electrons from energies between a few tens of keV and several MeV, corresponding to magnetic rigidities in the range 200 kV to a few MV, and protons with energies above 300 MeV (magnetic rigidities >800 MV). There is no evidence of a sequential rise in particle energy, as would be expected if a single acceleration process took minutes to get the particles to the high energies. Therefore the shock wave producing the early type II burst played no major role in this process. Radio emission of shock-accelerated electrons during the impulsive phase has also been observed with LOFAR at frequencies below 100 MHz (Morosan et al., 2019). The type II burst at these frequencies may be the continuation of the one displayed in **Figure 5A**. The authors use radio images to localize the acceleration region at the southern flank and near the summit of the CME (their Figure 3), far from the microwave sources seen by EOVS and the flaring active region. DH type III bursts observed by the STEREO A spacecraft between about 15:50 and 16:30 (not shown; see Figure 9 of Kocharov et al., 2020) demonstrate that at least electrons accelerated during the impulsive phase have access to open magnetic field lines. Unfortunately the Wind/WAVES spectrograph was not operating in the early phase of the event, so we cannot use the low-frequency behavior of the type III bursts to see whether the open field lines are connected to the Earth.

After the impulsive phase the microwave and hard X-ray emissions first decayed, as shown in the left panels of **Figure 4**. While RHESSI ceased observing, a second burst was seen in microwaves between 16:25 and 16:55, well after the



impulsive phase. The sources, displayed in the bottom right panel, were on the flanks of the flare loops seen in EUV, but still related to the plasma sheet above. Lack of microwave emission from the plasma sheet can be attributed to the weak magnetic field. The pion-decay gamma-rays (**Figure 6A**), as well as gamma-rays in the (0.8–7) MeV range (Figure 6 of Kurt et al., 2019), decayed after the impulsive peak together with the hard X-rays and microwaves, but stayed above the pre-event background. The gamma-ray flux showed a shallow new rise that accelerated at 16:25 UT, but the observations were interrupted by spacecraft night. When Fermi/LAT observed the Sun again, after 17:30, the flux had considerably decreased, but was still well above background. The start of the gamma-ray rise near 16:25 accompanied the rise of the second microwave burst (see also Kocharov et al., 2020). This and the decreased level observed after the spacecraft night suggest that the second microwave burst was accompanied by pion-decay gamma-ray emission, too.

The observations are very similar to the event on 2005 Jan 20, where a common rise of the hard X-ray, microwave and pion-decay gamma-ray emission was observed, with a time structure showing successive elementary bursts (**Figure 3B**). The hard X-ray and gamma-ray emission (at MeV energies) in that event also showed loop-top sources (Krucker et al., 2008), but

no microwave images or high-cadence EUV images were available in 2005. The scenario of coronal acceleration of high-energy protons and electrons in or around reconnecting current sheets in the impulsive and early post-impulsive phase is supported by both events. This phase lasted about an hour (15:50–16:50) on 2017 Sep 10.

Figure 6B compares the count rates of the first neutron monitor that sees solar particles (red; FSMT) and the average count rates of the other neutron monitors at high geomagnetic latitudes (Kurt et al., 2019). Because of the high latitude, the geomagnetic field does not affect the count rates considerably, and differences are essentially due to the anisotropy of the arriving particles. The similarity of time histories after 17 UT means that the arriving particles have an isotropic pitch-angle distribution. Before that time the particles reaching the Earth stream away from the Sun. The anisotropic phase hence gives an approximate idea of the time interval over which relativistic protons are released at the Sun. More details on the angular distribution are given by Mishev et al. (2018), and the interpretation using transport models is discussed in Kocharov et al. (2020). These authors conclude that the prompt component of the GLE lasts until 17:10 and is composed of protons arriving along the interplanetary magnetic field, while thereafter protons

from a different source, propagating across the magnetic field, dominate the neutron monitor count rates.

Kurt et al. (2019) took advantage of the GOES/HEPAD observations at energies above 700 MeV, and evaluated the arrival time of the first relativistic protons at Earth at $16:07 \pm 1$ min. They argued that this was consistent with a particle release at the Sun during the impulsive phase of the flare, which they estimate to occur between 15:59 and 16:01, near the peak of the impulsive-phase emission of the hard X-ray, gamma-ray, and microwave time profiles. Since the GLE is faint, and its rise slower than on 2005 Jan 20 (GLE 69), one may suppose that the actual onset was earlier than 16:07, but hidden in the background. The anisotropy of the GLE accompanies the impulsive rise and the delayed rise of the gamma-ray time profile in **Figure 6A**. The acceleration of the interacting and escaping relativistic protons seems to be closely correlated during the first hour of the event, and to be related with the mildly relativistic electrons emitting the microwave bursts in the low corona. These observations point toward a common acceleration in the current sheets formed behind the CME.

The extremely high speed of the CME observed during the event ($\sim 4,000 \text{ km s}^{-1}$) is also consistent with an early start of the particle release in a scenario of relativistic particle acceleration at the shock, proposed by Gopalswamy et al. (2018b) to start when the CME front is at a heliocentric distance of about $4 R_{\odot}$. The fast evolution of the impulsive early part of the gamma-ray emission shows that the protons are accelerated on faster time scales than expected at the CME shock. This is at least a strong argument against the shock being the accelerator of the first gamma-ray emitting protons in the impulsive flare phase. The overall correspondence of the anisotropic phase of the GLE with the radio emission from the flaring active region would have to be considered as coincidental if the CME shock were the accelerator of the relativistic protons. This GLE seems to support the idea that at least a large part of the relativistic protons come from impulsive and post-impulsive acceleration processes in the wake of the CME.

4 LONG-DURATION GAMMA-RAY EMISSION AND RADIO BURSTS

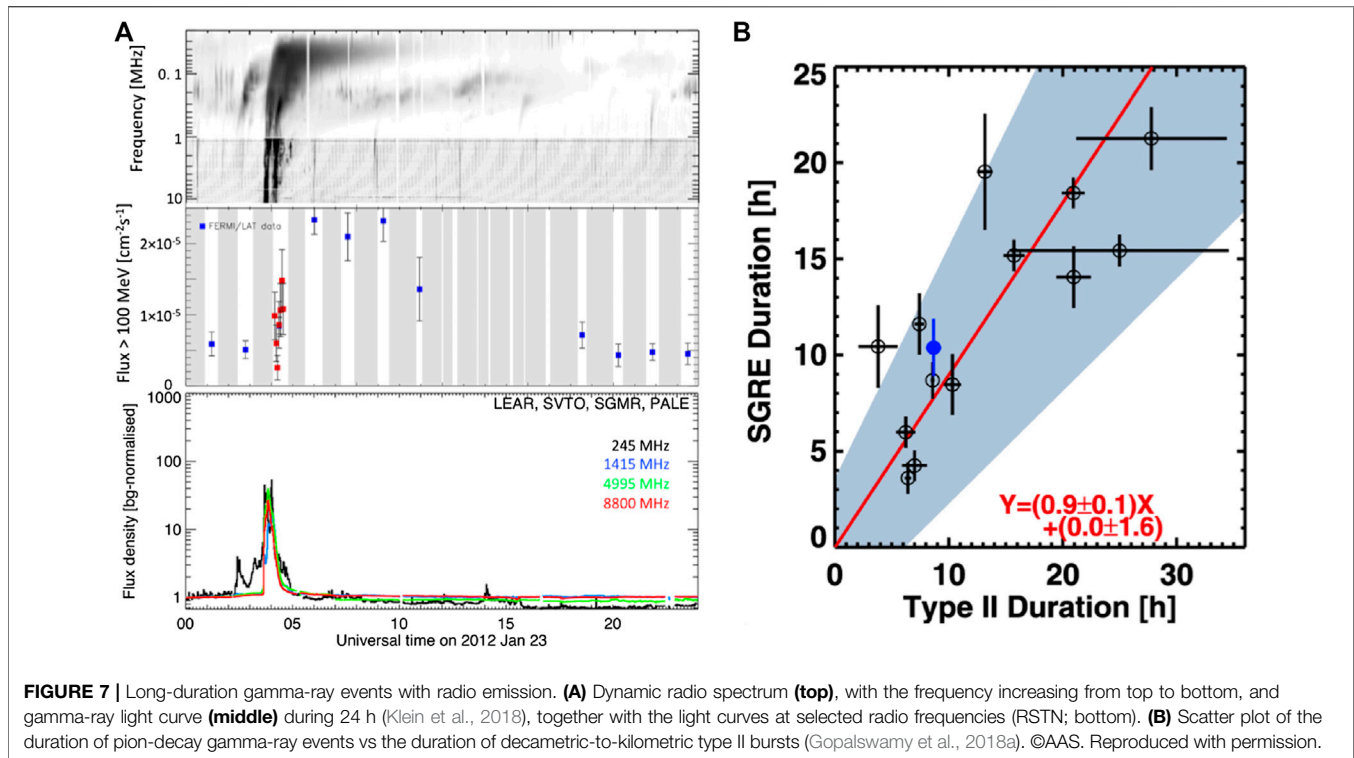
Gamma-ray bursts produced by pion-decay photons, where the pions themselves are produced by protons and α -particles with energies above 300 MeV, were occasionally detected since the 1990s (for a brief recent review, see *Section 2* of Klein et al., 2018). A major surprise of observations with the Fermi/LAT experiment was that pion-decay gamma-ray emission is far more frequent than GLEs, and that it may extend over much longer durations than hard X-ray or microwave signatures of mildly relativistic electrons interacting in the low solar atmosphere. Systematic investigations of Fermi/LAT gamma-ray events were conducted by Share et al. (2018) and Allafort (2018).

Klein et al. (2018) found that the long-duration gamma-ray events of Share et al. (2018) occur together with the long decay of soft X-ray emission and the formation of flare-loop arcades. With the exception of the first hour they had no radio counterpart at

centimetre-to-metre wavelengths. An example is shown in **Figure 7A**: a major radio burst lasting more than an hour (bottom panel) accompanied the early gamma-ray event (middle panel), but had decayed to background while the gamma-ray emission continued at a high level for several hours. So there was no signature of late electron acceleration at coronal heights below one solar radius, despite the substantial gamma-ray emission from high-energy protons. However, the gamma-ray events were found to be accompanied by decametric-to-hectometric type II bursts (DH type II bursts), as shown by the dynamic spectrum in the top panel. These shock signatures were seen during the entire time interval where the gamma-ray emission was enhanced. In a systematic analysis of the Fermi/LAT events Gopalswamy et al. (2018a) found that the durations of the type II bursts and the gamma-ray events were correlated, as shown by the scatter plot in **Figure 7B**. The authors concluded that this observation demonstrates that the relativistic protons emitting the gamma-rays were accelerated at the CME shock, together with the type II-burst emitting electrons. From the timing of the event in **Figure 7A** and the CME height-time plots in the SoHO/LASCO CME catalog (Yashiro et al., 2004)¹ the strongest gamma-ray emission occurred when the CME front was between 8 and $15 R_{\odot}$. The idea that the CME-driven shock was the accelerator of the gamma-ray emitting protons was substantiated by the demonstration of a magnetic connection from the shock to the chromosphere in several events (Plotnikov et al., 2017; Jin et al., 2018).

One aspect that is difficult to understand if the gamma-ray emitting protons are accelerated at the CME shock is how they can stream back from the shock to the chromosphere over $10\text{--}20 R_{\odot}$ against the magnetic mirror force, which would reflect all particles outside a tiny loss cone of width one degree or less (Mandzhavidze and Ramaty, 1992; Hudson, 2018; Klein et al., 2018). The gamma-ray event on 2017 Sep 10 stands out by the high flux during its long-duration phase (Omodei et al., 2018), together with an exceptionally high CME speed (Gopalswamy et al., 2018b). One consequence of the high CME speed is that the shock is far above the Sun at the time of the late-phase gamma-ray peak near 19:30, as far as $47 R_{\odot}$ as estimated in Figure 3F of Guo et al. (2018). In a standard magnetic field with an r^{-2} variation above a solar wind source surface with radius $2.5 R_{\odot}$ and an r^{-3} variation below, only particles with initial pitch angle $\leq 0.12^{\circ}$ would reach the chromosphere. The use of an undisturbed magnetic field model in this evaluation is of course not justified, since the ambient magnetic field around the outward propagating CME front will be compressed (see *Section 6.3* of Manchester et al., 2017, and references therein). But this does not remove the problem. Jin et al. (2018) postulated the existence of turbulence, which would continuously scatter protons into the loss cone. While high levels of turbulence in flaring magnetic structures in the low corona are plausible, where supporting spectroscopic observations exist (see Li et al., 2018; Polito et al., 2018; Warren et al., 2018, for the 2017 Sep 10 event), their presence in flux tubes extending over several tens of a solar radius along which relativistic protons would have to travel from

¹https://cdaw.gsfc.nasa.gov/CME_list/.



the shock front to the low solar atmosphere is a conjecture. Kocharov et al. (2020) argue that the acceleration region may be on the flank of the CME, but this again reduces the problem quantitatively without solving it. These objections add to those of de Nolfo et al. (2019) who argued against the idea of gamma-ray emission from backstreaming protons because they found no correlation between the numbers of protons in space and the numbers needed to explain the gamma-ray emission.

Another problem of the shock wave interpretation of gamma-ray events in the light of the study of Gopalswamy et al. (2018a) is that a common acceleration, with similar durations, of mildly relativistic protons and energetic electrons is not consistent with comparative analyses of electrons and protons at shocks in the heliosphere, where no closely correlated signatures are observed (see, e.g., Dresing et al., 2016). It is also generally believed that electrons emitting type II bursts are accelerated in very localized regions where the shock is quasi-perpendicular, while protons are supposed to be accelerated by diffusive shock acceleration, largely in the quasi-parallel regime. While the correlation between durations, and in some cases the comparable duration of DH type II bursts and long-duration gamma-ray events, is intriguing and needs to be understood, the direct interpretation as a common acceleration of the radio-emitting electrons and the gamma-ray emitting protons is not without problems.

An alternative interpretation is that there is no time-extended acceleration of protons during the entire duration of the gamma-ray event. Gamma-ray bursts lasting several hours were first observed by the Compton Gamma-Ray Telescope in 1991 (Kanbach et al., 1993). An early interpretation of this unusual duration was the trapping of relativistic protons, accelerated in

the early phase of a flare, in large coronal loops, from which they were thought to leak out gradually (Mandzhavidze and Ramaty, 1992). Their model calculations show that protons could survive in an arcade of coronal loops of height 10^7 m with ambient densities below $5 \cdot 10^{17} \text{ m}^{-3}$ and a very low level of waves to scatter the protons into the loss cone. The erupting flux rope itself is not a plausible long-term trap, because the protons would lose energy in the expanding structure. Taking again the 2017 Sep 10 event for illustration, the field-aligned momentum would decrease inversely as the height of the flux rope increases, i.e. by a factor of about 50 from the beginning of the eruption to the time of maximum of the long-duration gamma-ray emission. However, the arcade of flare loops forming in the wake of the CME has the required parameter range. The electron density of $5 \cdot 10^{15} \text{ m}^{-3}$ determined at the top of a flare loop arcade of the 2017 Sep 10 event by Cai et al. (2019) is consistent with the requirement of the model by Mandzhavidze and Ramaty (1992). This interpretation would not explain the observed relationship between the duration of the gamma-ray events and the type II bursts (Figure 7B). But it is noteworthy that in the 2017 Sep 10 event the duration of the gamma-ray emission exceeds by far that of the anisotropic phase of the GLE (Figure 6). The durations of both the radio emission and the anisotropic phase of the GLE are consistent with particle acceleration at the Sun during about an hour. This agrees qualitatively with a scenario of trapping and gradual release of the relativistic protons.

The acceleration of relativistic protons at shocks high in the corona has on the other hand the very attractive feature to explain why pion-decay gamma-ray emission may come from the photosphere while the flaring active region is at or behind the

solar limb. This is the case of the 2017 Sep 10 and several other events (Pesce-Rollins et al., 2015; Ackermann et al., 2017). The scenario receives strong support from data-driven CME and atmospheric modeling (Plotnikov et al., 2017) and MHD modeling (Jin et al., 2018) which shows that at relevant times the CME shock intercepts open field lines that are rooted in the earthward solar hemisphere. The source regions of electrons accelerated at the shock of the 2017 Sep 10 event, observed by LOFAR, were also localized at the CME flank connected to the earthward photosphere (Morosan et al., 2019, Figure 3). Grechnev et al. (2018) confront the scenarios of acceleration and trapping with a wealth of observations during the 2014 Sep 01 event, related with a flare at N14 E126. Their conclusion is that electrons emitting radio and hard X-rays are trapped in extended coronal loops, consistent with Ackermann et al. (2017), but that protons are also trapped there. They argue that the spectral hardening of the protons can be explained by re-acceleration, possibly by a shock wave, but that the particles are unlikely to stream back from the high corona.

5 CONCLUSION

The distinction between impulsive and gradual SEP events based on the role played by impulsive particle acceleration as in flares and CME shock acceleration is largely drawn from the association of the SEP events with radio emission: type III bursts as an example of impulsive electron acceleration, and type II bursts as a signature of coronal shock waves. The relatively low Mach numbers that many shocks emitting type II bursts probably have do not qualify them as efficient proton accelerators. The association of these bursts with SEP events may be spurious, due to the fact that the more energetic CMEs are more likely accompanied by some type II burst. But type II bursts do prove that a shock exists, and the trend that only CMEs accompanied by type II bursts have SEP events confirms the widely accepted idea that in “gradual” SEP events at energies ranging from hundreds of keV to some limit that lies well above 10 MeV a CME-driven shock is the dominant particle accelerator. Given the association of virtually all SEP events with type III bursts, particles accelerated in the corona in the wake of the CME can probably escape, and are likely to contribute to the SEP population in the early phase of the events.

Relativistic SEP events, on the other hand, have commonalities in their timing with radio emission both in the impulsive phase and the post-impulsive phase. This supports the idea that acceleration processes in the flaring active region and subsequently in higher regions in the wake of the rising CME make a major contribution to the SEP population. It is not excluded that the CME shock contributes also to relativistic SEPs. However, present indications that this is the case, based on the relative timing of relativistic SEPs and coronal acceleration signatures, are debatable. The onset delays observed in some events, which have been ascribed to the time needed by the shock-accelerated particles to become relativistic, have at least in some detailed studies been shown to have a common timing with type IV radio emission. The fact that type II emission starts before the gamma-ray emission of relativistic protons in the 2017 Sep 10 event is a counter-example to the claim

that the type II shock is an efficient accelerator at these energies. This is certainly not a definite answer, but the radio observations provide valuable arguments that the particle acceleration in solar eruptive events is more complex than the simple alternative between flare-accelerated impulsive events and CME-shock accelerated gradual events suggests.

The shock acceleration scenario, on the other hand, provides an easy explanation for the escape of SEPs to the Heliosphere, while particles accelerated in the wake of the CME are a priori confined in closed magnetic structures. However, the CME will interact with the surrounding coronal magnetic field, and this implies magnetic reconnection by which the accelerated particles can leak out (Masson et al., 2019). The presence of type III bursts in the eruptive events shows that open magnetic field lines do exist. While this process is plausible, observational evidence that it acts efficiently in SEP events still has to be established.

Radio observations remain an essential element for the scientific return of space missions dedicated to study SEPs and solar-terrestrial connections in general. The HELIOS mission demonstrated that observing energetic particles from vantage points close to the Sun reveals details in the time histories that are washed out once the particles reach 1 AU. The Parker Solar Probe and Solar Orbiter missions will provide new opportunities to understand the physical processes involved. The current wealth of radio instruments, unimaginable in the HELIOS era, will provide new insight into the nature of the radio sources. The powerful general purpose radio telescopes that can observe the Sun, such as the VLA, LOFAR, MWA and in the future SKA, can bring major new insight into the nature of the radio sources, as illustrated in *Section 3.1.3* of the companion chapter. The possibility of spectral imaging, i.e. obtaining an image at each frequency of the dynamic spectrum, is still largely unexploited because of the huge amount of data to be handled. Correcting the effects of radio wave propagation along paths that deviate from straight lines, due to ducting, refraction and scattering, will certainly become essential at some point (Duncan, 1979; Steinberg et al., 1984; Kontar et al., 2019). Currently, simplified models of the corona, such as a spherically symmetric background density, are employed, but models with increasingly detailed coronal density diagnostics should bring progress in this field.

But solar observing time with large multi-purpose instruments is restricted, and the large amounts of data are difficult and time-consuming to analyze. Dedicated solar patrol instruments continue to be needed, because only continuous observations ensure that all interesting events are captured. We need whole-Sun dynamic spectra, ideally from a worldwide network, for which e-Callisto (Benz et al., 2009) is a model. There is room to make these spectrographs more sensitive, but this must be done by individual groups worldwide. Radioheliographs at different places have provided much further insight and continue to produce essential observations. The major thread to ground-based radio astronomy is interference from terrestrial and space-borne emitters, which increasingly restrains the view of the radio sky. To some extent electronic and software procedures to reduce the interference can be developed, but agencies and operators should consider this issue in the allocation of frequencies. Solar radio monitoring also brings valuable information for space weather services, at relatively low cost.

Radio observations of the Sun continue to be needed - not only as a simple addition to the space missions, but to ensure their full scientific return. In solar physics the multi-messenger approach has been commonplace since three decades. Maintaining the relevant instruments is a wise use of resources and holds the promise of continuing discoveries into the future.

AUTHOR CONTRIBUTIONS

The author confirms being the sole contributor of this work and has approved it for publication.

ACKNOWLEDGMENTS

This work owes much to the generous data provision of numerous space-borne and ground-based instruments and data bases, especially the SoHO/LASCO CME catalog generated and maintained at the CDAW Data Center by NASA and The Catholic University of America in

REFERENCES

- Ackermann, M., Allafort, A., Baldini, L., Barbiellini, G., Bastieri, D., Bellazzini, R., et al. (2017). Fermi-LAT observations of high-energy behind-the-limb solar flares. *Astrophys. J.* 835, 219. doi:10.3847/1538-4357/835/2/219
- Afanasyev, A., Vainio, R., Rouillard, A. P., Battarbee, M., Aran, A., and Zucca, P. (2018). Modelling of proton acceleration in application to a ground level enhancement. *Astron. Astrophys.* 614, A4. doi:10.1051/0004-6361/201731343
- Akimov, V. V., Ambro, P., Below, A. V., Berlicki, A., Chertok, I. M., Karlický, M., et al. (1996). Evidence for prolonged acceleration based on a detailed analysis of the long-duration solar gamma-ray flare of June 15, 1991. *Sol. Phys.* 166, 107–134. doi:10.1007/BF00179358
- Allafort, A. (2018). High-energy gamma-ray observations of solar flares with the Fermi large area telescope. PhD thesis. Stanford (CA): Stanford University.
- Ameri, D., Valtonen, E., and Pohjolainen, S. (2019). Properties of high-energy solar particle events associated with solar radio emissions. *Sol. Phys.* 294, 122. doi:10.1007/s11207-019-1512-9
- Bale, S. D., Reiner, M. J., Bougeret, J.-L., Kaiser, M. L., Krucker, S., Larson, D. E., et al. (1999). The source region of an interplanetary type II radio burst. *Geophys. Res. Lett.* 26, 1573–1576. doi:10.1029/1999GL900293
- Bastian, T. S. (2007). Synchrotron radio emission from a fast halo coronal mass ejection. *Astrophys. J.* 665, 805–812. doi:10.1086/519246
- Benz, A. O., Monstein, C., Meyer, H., Manoharan, P. K., Ramesh, R., Altyntsev, A., et al. (2009). A world-wide net of solar radio spectrometers: e-CALLISTO. *Earth Moon Planets.* 104, 277–285. doi:10.1007/s11038-008-9267-6
- Benz, A. O., and Thejappa, G. (1988). Radio emission of coronal shock waves. *Astron. Astrophys.* 202, 267–274.
- Bouratzis, C., Preka-Papadema, P., Hillaris, A., Tsitsipis, P., Kontogeorgos, A., Kurt, V. G., et al. (2010). Radio observations of the January 20, 2005 extreme event. *Sol. Phys.* 267, 343–359. doi:10.1007/s11207-010-9648-7
- Bruno, A., Bazilevska, G. A., Boezio, M., Christian, E. R., de Nolfo, G. A., Martucci, M., et al. (2018). Solar energetic particle events observed by the PAMELA mission. *Astrophys. J.* 862, 97. doi:10.3847/1538-4357/aacc26
- Bruno, A. (2017). Calibration of the GOES 13/15 high-energy proton detectors based on the PAMELA solar energetic particle observations. *Space Weather.* 15, 1191–1202. doi:10.1002/2017SW001672
- Burgess, D. (2007). “Particle acceleration at the Earth’s bow shock,” in *The high energy solar corona: waves, eruptions, particles*. Editors K.-L. Klein and A. L. MacKinnon (Berlin, Germany: Springer Verlag), Vol. 725, 161–190.
- cooperation with the Naval Research Laboratory (https://cdaw.gsfc.nasa.gov/CME_list/), the Radio Monitoring web site (<http://secchirh.obspm.fr/>) at LESIA, Observatoire de Paris, supported by the French Space Agency CNES, the neutron monitor database (www.nmdb.eu) maintained at the University of Kiel and built within a Framework seven project of the European Union, and the National Centers for Environmental Information at NOAA (<https://www.ngdc.noaa.gov/stp/space-weather/solar-data>). The author acknowledges helpful discussions with many colleagues during the NMDB, SEPServer and HESPERIA projects funded by the European Union, during several working groups and workshops dedicated to solar energetic particles at the International Space Science Institute (ISSI) in Bern, and during workshops of the Community of European Solar Radio Astronomers (CESRA). He is indebted to the referees for their patient and constructive criticism. This research was supported by the French Polar Institute (IPEV), space agency (CNES), and Programme National Soleil-Terre (PNST) of CNRS/INSU.
- Bütikofer, R. (2018). “Ground-based measurements of energetic particles by neutron monitors,” in *Solar particle radiation storms forecasting and analysis*. Editors O. E. Malandraki and N. B. Crosby, 444, 95–112. doi:10.1007/978-3-319-60051-2_6
- Cai, Q., Shen, C., Raymond, J. C., Mei, Z., Warmuth, A., Roussev, I. I., et al. (2019). Investigations of a supra-arcade fan and termination shock above the top of the flare-loop system of the 2017 September 10 event. *Mon. Not. Roy. Astron. Soc.* 489, 3183–3199. doi:10.1093/mnras/stz2167
- Cairns, I. H. (2011). “Coherent radio emissions associated with solar system shocks,” in *The Sun, the solar wind, and the heliosphere*. Editors M. P. Miralles and J. Sánchez Almeida (Berlin, Germany: Springer), Vol. 4, 267–338.
- Cairns, I. H., and Robinson, R. D. (1987). Herringbone bursts associated with type II solar radio emission. *Sol. Phys.* 111 (2), 365–383. doi:10.1007/bf00148526
- Cane, H. V., Erickson, W. C., and Prestage, N. P. (2002). Solar flares, type III radio bursts, coronal mass ejections and energetic particles. *J. Geophys. Res.* 107, 1315. doi:10.1029/2001JA000320
- Cane, H. V., and Erickson, W. C. (2005). Solar type II radio bursts and IP type II events. *Astrophys. J.* 623, 1180–1194. doi:10.1086/428820
- Cane, H. V., Stone, R. G., Fainberg, J., Steinberg, J. L., Hoang, S., and Stewart, R. T. (1981). Radio evidence for shock acceleration of electrons in the solar corona. *Geophys. Res. Lett.* 8, 1285–1288. doi:10.1029/GL008i12p01285
- Cane, H. V., and Stone, R. G. (1984). Type II solar radio bursts, interplanetary shocks, and energetic particle events. *Astrophys. J.* 282, 339–344. doi:10.1086/162207
- Carley, E. P., Vilmer, N., Simões, P. J. A., and Ó Ferraigh, B. (2017). Estimation of a coronal mass ejection magnetic field strength using radio observations of gyrosynchrotron radiation. *Astron. Astrophys.* 608, A137. doi:10.1051/0004-6361/201731368
- Cho, K.-S., Lee, J., Gary, D. E., Moon, Y.-J., and Park, Y. D. (2007). Magnetic field strength in the solar corona from type II band splitting. *Astrophys. J.* 665, 799–804. doi:10.1086/519160
- Claßen, H. T., and Aurass, H. (2002). On the association between type II radio bursts and CMEs. *Astron. Astrophys.* 384 (3), 1098–1106. doi:10.1051/0004-6361:20020092
- Cliver, E. W., Dennis, B. R., Kiplinger, A. L., Kane, S. R., Neidig, D. F., Sheeley, N. R., et al. (1986). Solar gradual hard X-ray bursts and associated phenomena. *Astrophys. J.* 305, 920–935. doi:10.1086/164306
- Cliver, E. W., Kahler, S. W., and Reames, D. V. (2004). Coronal shocks and solar energetic proton events. *Astrophys. J.* 605, 902–910. doi:10.1086/382651

- Cliver, E. W., and Ling, A. G. (2009). Low-frequency type III bursts and solar energetic particle events. *Astrophys. J.* 690, 598–609. doi:10.1088/0004-637X/690/1/598
- Dauphin, C., Vilmer, N., and Krucker, S. (2006). Observations of a soft X-ray rising loop associated with a type II burst and a coronal mass ejection in the 03 November 2003 X-ray flare. *Astron. Astrophys.* 455, 339–348. doi:10.1051/0004-6361:20054535
- Dauphin, C., Vilmer, N., Lüthi, T., Trotter, G., Krucker, S., and Magun, A. (2005). Modulations of broad-band radio continua and X-ray emissions in the large X-ray flare on 03 November 2003. *Adv. Space Res.* 35, 1805–1812. doi:10.1016/j.asr.2005.04.092
- de Nolfo, G. A., Bruno, A., Ryan, J. M., Dalla, S., Giacalone, J., Richardson, I. G., et al. (2019). Comparing long-duration gamma-ray flares and high-energy solar energetic particles. *Astrophys. J.* 879, 90. doi:10.3847/1538-4357/ab258f
- Dresing, N., Theesen, S., Klassen, A., and Heber, B. (2016). Efficiency of particle acceleration at interplanetary shocks: statistical study of STEREO observations. *Astron. Astrophys.* 588, A17. doi:10.1051/0004-6361/201527853
- Du, G., Kong, X., Chen, Y., Feng, S., Wang, B., and Li, G. (2015). An observational revisit of band-split solar type-II radio bursts. *Astrophys. J.* 812, 52. doi:10.1088/0004-637X/812/1/52
- Dulk, G. A., Leblanc, Y., Bastian, T. S., and Bougeret, J. L. (2000). Acceleration of electrons at type II shock fronts and production of shock-accelerated type III bursts. *J. Geophys. Res.* 105, 27343–27352.
- Duncan, R. A. (1979). Wave ducting of solar metre-wave radio emission as an explanation of fundamental/harmonic source coincidence and other anomalies. *Sol. Phys.* 63, 389–398. doi:10.1007/BF00174543
- Fitzenreiter, R. J., Ogilvie, K. W., Bale, S. D., and Viñas, A. F. (2003). Modification of the solar wind electron velocity distribution at interplanetary shocks. *J. Geophys. Res.* 108, 1415. doi:10.1029/2003JA009865
- Gary, D. E., Chen, B., Dennis, B. R., Fleishman, G. D., Hurford, G. J., Krucker, S., et al. (2018). Microwave and hard X-ray observations of the 2017 September 10 solar limb flare. *Astrophys. J.* 863, 83. doi:10.3847/1538-4357/aad0ef
- Gopalswamy, N., Aguilar-Rodriguez, E., Yashiro, S., Nunes, S., Kaiser, M. L., and Howard, R. A. (2005). Type II radio bursts and energetic solar eruptions. *J. Geophys. Res.* 110, A12S07. doi:10.1029/2005JA011158
- Gopalswamy, N. (2009). “Coronal mass ejections and space weather,” in *Climate and weather of the sun-earth system (CAWSES) selected papers from the 2007 kyoto symposium*. Editors T. Tsuda, R. Fujii, K. Shibata, and M. A. Geller (Tokyo (Japan): TERRAPUB), 77–120.
- Gopalswamy, N., Mäkelä, P., Yashiro, S., Lara, A., Xie, H., Akiyama, S., et al. (2018a). Interplanetary type II radio bursts from Wind/WAVES and sustained gamma-ray emission from Fermi/LAT: evidence for shock source. *Astrophys. J. Lett.* 868, L19. doi:10.3847/2041-8213/aaef36
- Gopalswamy, N., Xie, H., Mäkelä, P., Yashiro, S., Akiyama, S., Uddin, W., et al. (2013). Height of shock formation in the solar corona inferred from observations of type II radio bursts and coronal mass ejections. *Adv. Space Res.* 51, 1981–1989. doi:10.1016/j.asr.2013.01.006
- Gopalswamy, N., Xie, H., Yashiro, S., Akiyama, S., Mäkelä, P., and Usoskin, I. G. (2012). Properties of Ground Level Enhancement events and the associated solar eruptions during solar cycle 23. *Space Sci. Rev.* 171, 23–60. doi:10.1007/s11214-012-9890-4
- Gopalswamy, N., Yashiro, S., Akiyama, S., Mäkelä, P., Xie, H., Kaiser, M. L., et al. (2008a). Coronal mass ejections, type II radio bursts, and solar energetic particle events in the SOHO era. *Ann. Geophys.* 26, 3033–3047. doi:10.5194/angeo-26-3033-2008
- Gopalswamy, N., Yashiro, S., Mäkelä, P., Xie, H., Akiyama, S., and Monstein, C. (2018b). Extreme kinematics of the 2017 September 10 solar eruption and the spectral characteristics of the associated energetic particles. *Astrophys. J. Lett.* 863, L39. doi:10.3847/2041-8213/aad86c
- Gopalswamy, N., Yashiro, S., Michalek, G., Kaiser, M. L., Howard, R. A., Reames, D. V., et al. (2002). Interacting coronal mass ejections and solar energetic particles. *Astrophys. J. Lett.* 572, L103–L107. doi:10.1086/341601
- Gopalswamy, N., Yashiro, S., Xie, H., Akiyama, S., Aguilar-Rodriguez, E., Kaiser, M. L., et al. (2008b). Radio-quiet fast and wide coronal mass ejections. *Astrophys. J.* 674, 560–569. doi:10.1086/524765
- Grechnev, V. V., Kiselev, V. I., Kashapova, L. K., Kochanov, A. A., Zimovets, I. V., Uralov, A. M., et al. (2018). Radio, hard X-ray, and gamma-ray emissions associated with a far-side solar event. *Sol. Phys.* 293, 133. doi:10.1007/s11207-018-1352-z
- Grechnev, V. V., Kurt, V. G., Chertok, I. M., Uralov, A. M., Nakajima, H., Altyntsev, A. T., et al. (2008). An extreme solar event of 20 January 2005: properties of the flare and the origin of energetic particles. *Sol. Phys.* 252, 149–177. doi:10.1007/s11207-008-9245-1
- Guo, J., Dumbović, M., Wimmer-Schweingruber, R. F., Temmer, M., Lohf, H., Wang, Y., et al. (2018). Modeling the evolution and propagation of 10 September 2017 CMEs and SEPs arriving at Mars constrained by remote sensing and *in situ* measurement. *Space Weather.* 16, 1156–1169. doi:10.1029/2018SW001973
- Holman, G. D., and Pesses, M. E. (1983). Solar type II radio emission and the shock drift acceleration of electrons. *Astrophys. J.* 267, 837–843. doi:10.1086/160918
- Hudson, H. S. (2018). “The relationship between long-duration gamma-ray flares and solar cosmic rays,” in *Space weather of the heliosphere: processes and forecasts*. Editors C. Foullon and O. E. Malandraki (Vienna, Austria: IAU Symposium), Vol. 335, 49–53. doi:10.1017/S1743921317009681
- Iwai, K., Yashiro, S., Nitta, N. V., and Kubo, Y. (2020). Spectral structures of type II solar radio bursts and solar energetic particles. *Astrophys. J.* 888, 50. doi:10.3847/1538-4357/ab57ff
- Janvier, M., Aulanier, G., and Démoulin, P. (2015). From coronal observations to MHD simulations, the building blocks for 3D models of solar flares (Invited Review). *Sol. Phys.* 290, 3425–3456. doi:10.1007/s11207-015-0710-3
- Jebbaraj, I. C., Magdalenic, J., Podladchikova, T., Scolini, C., Pomoell, J., Veronig, A. M., et al. (2020). Using radio triangulation to understand the origin of two subsequent type II radio bursts. *Astron. Astrophys.* 639, A56. doi:10.1051/0004-6361/201937273
- Jin, M., Petrosian, V., Liu, W., Nitta, N. V., Omodei, N., Rubio da Costa, F., et al. (2018). Data-driven simulations of magnetic connectivity in behind-the-limb γ -ray flares and associated coronal mass ejections. *Astrophys. J.* 867 (2), 122. doi:10.3847/1538-4357/aae1fd
- Kahler, S. (1994). Injection profiles of solar energetic particles as functions of coronal mass ejection heights. *Astrophys. J.* 428, 837–842. doi:10.1086/174292
- Kahler, S. W. (1982a). Radio burst characteristics of solar proton flares. *Astrophys. J.* 261, 710–719. doi:10.1086/160381
- Kahler, S. W. (1982b). The role of the big flare syndrome in correlations of solar energetic proton fluxes and associated microwave burst parameters. *J. Geophys. Res.* 87, 3439–3448. doi:10.1029/JA087iA05p03439
- Kanbach, G., Bertsch, D. L., Fichtel, C. E., Hartman, R. C., Hunter, S. D., Kniffen, D. A., et al. (1993). Detection of a long-duration solar gamma-ray flare on June 11, 1991 with EGRET on COMPTON-GRO. *Astron. Astrophys. Suppl.* 97, 349–353.
- Kerdraon, A., Pick, M., Hoang, S., Wang, Y., and Haggerty, D. (2010). The coronal and heliospheric 2007 May 19 event: coronal mass ejection, Extreme Ultraviolet Imager wave, radio bursts, and energetic electrons. *Astrophys. J.* 715 (1), 468–476. doi:10.1088/0004-637X/715/1/468
- Kishore, P., Ramesh, R., Hariharan, K., Kathiravan, C., and Gopalswamy, N. (2016). Constraining the solar coronal magnetic field strength using split-band type II radio burst observations. *Astrophys. J.* 832, 59. doi:10.3847/0004-637X/832/1/59
- Klassen, A., Bothmer, V., Mann, G., Reiner, M. J., Krucker, S., Vourlidis, A., et al. (2002). Solar energetic electron events and coronal shocks. *Astron. Astrophys.* 385 (3), 1078–1088. doi:10.1051/0004-6361:20020205
- Klassen, A., Pohjolainen, S., and Klein, K.-L. (2003). Type II radio precursor and X-ray flare emission. *Sol. Phys.* 218, 197–210. doi:10.1023/b:sola.0000013034.61996.c4
- Klein, K.-L., Agueda, N., and Bütikofer, R. (2015). “On the origin of relativistic solar particle events: interplanetary transport modelling and radio emission,” in *Proceedings of science 34th international cosmic ray conference*. Editors R. Caballero, J. C. D’Olivo, G. Medina-Tanco, L. Nellen, F. A. Sánchez, and J. F. Valdés-Galicia, Hague, Netherlands, July 30–August 6, 2015. 121–124.
- Klein, K.-L., Chupp, E. L., Trotter, G., Magun, A., Dunphy, P. P., Rieger, E., et al. (1999a). Flare-associated energetic particles in the corona and at 1 AU. *Astron. Astrophys.* 348, 271–285.
- Klein, K.-L., Khan, J. I., Vilmer, N., Delouis, J., and Aurass, H. (1999b). X-ray and radio evidence on the origin of a coronal shock wave. *Astron. Astrophys.* 346, L53–L56.
- Klein, K.-L., Masson, S., Bouratzis, C., Grechnev, V., Hillaris, A., and Preka-Papadema, P. (2014). The relativistic solar particle event of 2005 January 20: origin of delayed particle acceleration. *Astron. Astrophys.* 572, A4. doi:10.1051/0004-6361/201423783

- Klein, K.-L., and Trotter, G. (1994). "Energetic electron injection into the high corona during the gradual phase of flares: evidence against acceleration by a large scale shock," in AIP conference Proceedings 294: high-energy solar phenomena - a new era of spacecraft measurements. Editors J. Ryan and W. Veststrand, Waterville Valley, NH, December 10, 1994, 187. doi:10.1063/1.45183
- Klein, K.-L., Tziotziou, K., Zucca, P., Valtonen, E., Vilmer, N., Malandraki, O. E., et al. (2018). "X-ray, radio and SEP observations of relativistic gamma-ray events," in *Solar particle radiation storms forecasting and analysis*. Editors O. E. Malandraki and N. B. Crosby (Berlin, Germany: Springer), Vol. 444 133–155. doi:10.1007/978-3-319-60051-2_8
- Kocharov, L., Pesce-Rollins, M., Laitinen, T., Mishev, A., K uhl, P., Klassen, A., et al. (2020). Interplanetary protons versus interacting protons in the 2017 September 10 solar eruptive event. *Astrophys. J.* 890, 13. doi:10.3847/1538-4357/ab684e
- Kontar, E. P., Chen, X., Chrysaphi, N., Jeffrey, N. L. S., Emslie, A. G., Krupar, V., et al. (2019). Anisotropic radio-wave scattering and the interpretation of solar radio emission observations. *Astrophys. J.* 884, 122. doi:10.3847/1538-4357/ab40bb
- Kouloumvakos, A., Nindos, A., Valtonen, E., Alissandrakis, C. E., Malandraki, O., Tsiotis, P., et al. (2015). Properties of solar energetic particle events inferred from their associated radio emission. *Astron. Astrophys.* 580, A80. doi:10.1051/0004-6361/201424397
- Kouloumvakos, A., Rouillard, A. P., Wu, Y., Vainio, R., Vourlidis, A., Plotnikov, I., et al. (2019). Connecting the properties of coronal shock waves with those of solar energetic particles. *Astrophys. J.* 876, 80. doi:10.3847/1538-4357/ab15d7
- Kozarev, K. A., Dayeh, M. A., and Farahat, A. (2019). Early-stage solar energetic particle acceleration by coronal mass ejection-driven shocks with realistic seed spectra. I. Low corona. *Astrophys. J.* 871, 65. doi:10.3847/1538-4357/aaf1ce
- Krucker, S., Hurford, G. J., MacKinnon, A. L., Shih, A. Y., and Lin, R. P. (2008). Coronal γ -ray bremsstrahlung from solar flare-accelerated electrons. *Astrophys. J. Lett.* 678, L63–L66. doi:10.1086/588381
- K uhl, P., Dresing, N., Heber, B., and Klassen, A. (2017). Solar Energetic particle events with protons above 500 MeV between 1995 and 2015 measured with SOHO/EPHIN. *Sol. Phys.* 292, 10. doi:10.1007/s11207-016-1033-8
- Kundu, M. R., MacDowall, R. J., and Stone, R. G. (1990). Kilometric shock-associated events and microwave bursts. *Astrophys. Space Sci.* 165, 101–110. doi:10.1007/BF00653661
- Kurt, V., Belov, A., Kudela, K., Mavromichalaki, H., Kashapova, L., Yushkov, B., et al. (2019). Onset time of the GLE 72 observed at neutron monitors and its relation to electromagnetic emissions. *Sol. Phys.* 294, 22. doi:10.1007/s11207-019-1407-9
- Kuznetsov, S. N., Kurt, V. G., Yushkov, B. Y., and Kudela, K. (2008). "CORONAS-F satellite data on the delay between the proton acceleration on the Sun and their detection at 1 AU," 30th international cosmic ray conference. Editors R. Caballero, J. C. D'Olivo, G. Medina-Tanco, L. Nellen, F. A. S anchez, and J. F. Vald es, 1 (Mexico City, Mexico: Universidad Nacional Aut onoma de M xico). 121–124.
- Kwon, R.-Y., and Vourlidis, A. (2018). The density compression ratio of shock fronts associated with coronal mass ejections. *Journal of Space Weather and Space Climate.* 8, A08. doi:10.1051/swsc/2017045
- Li, Y., Xue, J. C., Ding, M. D., Cheng, X., Su, Y., Feng, L., et al. (2018). Spectroscopic observations of a current sheet in a solar flare. *Astrophys. J. Lett.* 853, L15. doi:10.3847/2041-8213/aaa6c0
- Magdalenic, J., Marqu e, C., Krupar, V., Mierla, M., Zhukov, A. N., Rodriguez, L., et al. (2014). Tracking the CME-driven shock wave on 2012 March 5 and radio triangulation of associated radio emission. *Astrophys. J.* 791, 115. doi:10.1088/0004-637X/791/2/115
- Magdalenic, J., Marqu e, C., Zhukov, A. N., Vr snak, B., and Veronig, A. (2012). Flare-generated type II burst without associated coronal mass ejection. *Astrophys. J.* 746, 152. doi:10.1088/0004-637X/746/2/152
- Maguire, C. A., Carley, E. P., McCauley, J., and Gallagher, P. T. (2020). Evolution of the Alfv en Mach number associated with a coronal mass ejection shock. *A&A.* 633, A56. doi:10.1051/0004-6361/201936449
- Manchester, W., Kilpua, E. K. J., Liu, Y. D., Lugaz, N., Riley, P., T or k, T., et al. (2017). The physical processes of CME/ICME evolution. *Space Sci. Rev.* 212, 1159–1219. doi:10.1007/s11214-017-0394-0
- Mancuso, S. (2007). Coronal transients and metric type II radio bursts. II. Accelerations at low coronal heights. *Astron. Astrophys.* 463, 1137–1141. doi:10.1051/0004-6361:20054767
- Mancuso, S., and Avetta, D. (2008). UV and radio observations of the coronal shock associated with the 2002 July 23 coronal mass ejection event. *Astrophys. J.* 677, 683–691. doi:10.1086/528839
- Mancuso, S., and Garzelli, M. V. (2013). Coronal magnetic field strength from Type II radio emission: complementarity with Faraday rotation measurements. *Astron. Astrophys.* 560, L1. doi:10.1051/0004-6361/201322645
- Mandzhavidze, N., and Ramaty, R. (1992). Gamma rays from pion decay - evidence for long-term trapping of particles in solar flares. *Astrophys. J. Lett.* 396, L111–L114. doi:10.1086/186529
- Mann, G., Classen, T., and Aurass, H. (1995). Characteristics of coronal shock waves and solar type II radio bursts. *Astron. Astrophys.* 295, 775–781.
- Mann, G., and Klassen, A. (2005). Electron beams generated by shock waves in the solar corona. *Astron. Astrophys.* 441, 319–326. doi:10.1051/0004-6361:20034396
- Mann, G., Melnik, V. N., Rucker, H. O., Konovalenko, A. A., and Brazhenko, A. I. (2018). Radio signatures of shock-accelerated electron beams in the solar corona. *Astron. Astrophys.* 609, A41. doi:10.1051/0004-6361/201730546
- Masson, S., Antiochos, S. K., and DeVore, C. R. (2019). Escape of flare-accelerated particles in solar eruptive events. *Astrophys. J.* 884, 143. doi:10.3847/1538-4357/ab4515
- Masson, S., Klein, K.-L., B utikofer, R., Fl uckiger, E. O., Kurt, V., Yushkov, B., et al. (2009). Acceleration of relativistic protons during the 20 January 2005 flare and CME. *Sol. Phys.* 257, 305–322. doi:10.1007/s11207-009-9377-y
- McCracken, K. G., Moraal, H., and Shea, M. A. (2012). The high-energy impulsive ground-level enhancement. *Astrophys. J.* 761, 101. doi:10.1088/0004-637X/761/2/101
- McCracken, K. G., Moraal, H., and Stoker, P. H. (2008). Investigation of the multiple-component structure of the 20 January 2005 cosmic ray ground level enhancement. *J. Geophys. Res.* 113, 12101. doi:10.1029/2007JA012829
- Miroshnichenko, L. I. (2001). *Solar cosmic rays*. Dordrecht/Boston/London: Kluwer Acad. Publishing.
- Mishev, A., Usoskin, I., Raukunen, O., Paasilta, M., Valtonen, E., Kocharov, L., et al. (2018). First analysis of ground-level enhancement (GLE) 72 on 10 September 2017: spectral and anisotropy characteristics. *Sol. Phys.* 293, 136. doi:10.1007/s11207-018-1354-x
- Moraal, H., and Caballero-Lopez, R. A. (2014). The cosmic-ray ground-level enhancement of 1989 September 29. *Astrophys. J.* 790, 154. doi:10.1088/0004-637X/790/2/154
- Moraal, H., and McCracken, K. G. (2012). The time structure of Ground Level Enhancements in solar cycle 23. *Space Sci. Rev.* 171, 85–95. doi:10.1007/s11214-011-9742-7
- Morosan, D. E., Carley, E. P., Hayes, L. A., Murray, S. A., Zucca, P., Fallows, R. A., et al. (2019). Multiple regions of shock-accelerated particles during a solar coronal mass ejection. *Nature Astronomy.* 3, 452–461. doi:10.1038/s41550-019-0689-z
- Muhr, N., Veronig, A. M., Kienreich, I. W., Temmer, M., and Vr snak, B. (2011). Analysis of characteristic parameters of large-scale coronal waves observed by the Solar-Terrestrial Relations Observatory/Extreme Ultraviolet Imager. *Astrophys. J.* 739, 89. doi:10.1088/0004-637X/739/2/89
- Nindos, A., Alissandrakis, C. E., Hillaris, A., and Preka-Papadema, P. (2011). On the relationship of shock waves to flares and coronal mass ejections. *Astron. Astrophys.* 531, A31. doi:10.1051/0004-6361/201116799
- Omodei, N., Pesce-Rollins, M., Longo, F., Allafort, A., and Krucker, S. (2018). Fermi-LAT observations of the 2017 September 10 solar flare. *Astrophys. J. Lett.* 865, L7. doi:10.3847/2041-8213/aae077
- Pesce-Rollins, M., Omodei, N., Petrosian, V., Liu, W., Rubio da Costa, F., Allafort, A., et al. (2015). First detection of 100 MeV gamma-rays associated with a behind-the-limb solar flare. *Astrophys. J. Lett.* 805, L15. doi:10.1088/2041-8205/805/2/L15
- Pick, M., D emoulin, P., Krucker, S., Malandraki, O., and Maia, D. (2005). Radio and X-ray signatures of magnetic reconnection behind an ejected flux rope. *Astrophys. J.* 625, 1019–1026. doi:10.1086/429530
- Plotnikov, I., Rouillard, A. P., and Share, G. H. (2017). The magnetic connectivity of coronal shocks from behind-the-limb flares to the visible solar surface during γ -ray events. *Astron. Astrophys.* 608, A43. doi:10.1051/0004-6361/201730804
- Pohjolainen, S., Allawi, H., and Valtonen, E. (2013). Origin of wide-band IP type II bursts. *Astron. Astrophys.* 558, A7. doi:10.1051/0004-6361/201220688
- Pohjolainen, S., van Driel-Gesztelyi, L., Culhane, J. L., Manoharan, P. K., and Elliott, H. A. (2007). CME propagation characteristics from radio observations. *Sol. Phys.* 244, 167–188. doi:10.1007/s11207-007-9006-6
- Polito, V., Dudik, J., Ka sparova, J., Dzijfakova, E., Reeves, K. K., Testa, P., et al. (2018). Broad non-Gaussian Fe XXIV line profiles in the impulsive phase of the 2017 September 10 X8.3-class flare observed by Hinode/EIS. *Astrophys. J.* 864, 63. doi:10.3847/1538-4357/aad62d

- Pulupa, M., and Bale, S. D. (2008). Structure on interplanetary shock fronts: type II radio burst source regions. *Astrophys. J.* 676, 1330–1337. doi:10.1086/526405
- Reames, D. V. (1999). Particle acceleration at the sun and in the heliosphere. *Space Sci. Rev.* 90, 413–491. doi:10.1023/A:1005105831781
- Reames, D. V. (2009). Solar release times of energetic particles in Ground-Level Events. *Astrophys. J.* 693, 812–821. doi:10.1088/0004-637X/693/1/812
- Reiner, M. J., Kaiser, M. L., Gopalswamy, N., Aurass, H., Mann, G., Vourlidis, A., et al. (2001). Statistical analysis of coronal shock dynamics implied by radio and white-light observations. *J. Geophys. Res.* 106, 25279–25290. doi:10.1029/2000JA004024
- Reiner, M. J., Karlický, M., Jiika, K., Aurass, H., et al. (2000). On the solar origin of complex type III-like radio bursts observed at and below 1 MHz. *Astrophys. J.* 530, 1049–1060. doi:10.1086/308394
- Reiner, M. J., Klein, K.-L., Karlický, M., Jiříčka, K., Klassen, A., Kaiser, M. L., et al. (2008). Solar origin of the radio attributes of a complex type III burst observed on 11 April 2001. *Sol. Phys.* 249, 337–354. doi:10.1007/s11207-008-9189-5
- Reiner, M. J., Krucker, S., Gary, D. E., Dougherty, B. L., Kaiser, M. L., and Bougeret, J.-L. (2007). Radio and white-light coronal signatures associated with the RHESSI hard X-ray event of 2002 July 23. *Astrophys. J.* 657, 1107–1116. doi:10.1086/510827
- Richardson, I. G., von Roseninge, T. T., Cane, H. V., Christian, E. R., Cohen, C. M. S., Labrador, A. W., et al. (2014). 25 MeV proton events observed by the High Energy Telescopes on the STEREO A and B spacecraft and/or at Earth during the first seven years of the STEREO mission. *Sol. Phys.* 289, 3059–3107. doi:10.1007/s11207-014-0524-8
- Rouillard, A. P., Plotnikov, I., Pinto, R. F., Tirole, M., Lavarra, M., Zucca, P., et al. (2016). Deriving the properties of coronal pressure fronts in 3D: application to the 2012 May 17 ground level enhancement. *Astrophys. J.* 833, 45. doi:10.3847/1538-4357/833/1/45
- Salas-Matamoros, C., Klein, K.-L., and Rouillard, A. P. (2016). Coronal mass ejection-related particle acceleration regions during a simple eruptive event. *Astron. Astrophys.* 590, A135. doi:10.1051/0004-6361/201528015
- Seaton, D., and Darnel, J. (2018). Observations of an eruptive solar flare in the extended EUV solar corona. *Astrophys. J. Lett.* 852. doi:10.3847/2041-8213/aaa28e
- Shanmugaraju, A., Bendict Lawrance, M., Moon, Y. J., Lee, J.-O., and Suresh, K. (2017). Heights of coronal mass ejections and shocks inferred from metric and DH type II radio bursts. *Sol. Phys.* 292, 136. doi:10.1007/s11207-017-1155-7
- Share, G. H., Murphy, R. J., White, S. M., Tolbert, A. K., Dennis, B. R., Schwartz, R. A., et al. (2018). Characteristics of late-phase 100 MeV gamma-ray emission in solar eruptive events. *Astrophys. J.* 869, 182. doi:10.3847/1538-4357/aabf7
- Smerd, S. F., Sheridan, K. V., and Stewart, R. T. (1975). Split-band structure in type II radio bursts from the Sun. *Astrophys. J. Lett.* 16, 23–28.
- Steinberg, J. L., Hoang, S., Lecacheux, A., Aubier, M. G., and Dulk, G. A. (1984). Type III radio bursts in the interplanetary medium - the role of propagation. *Astron. Astrophys.* 140, 39–48.
- Stewart, R. T., and Magun, A. (1980). Radio evidence for electron acceleration by transverse shock waves in herringbone Type II solar bursts. *Pub. Astron. Soc. Australia.* 4, 53–55.
- Su, W., Cheng, X., Ding, M. D., Chen, P. F., and Sun, J. Q. (2015). A type II radio burst without a coronal mass ejection. *Astrophys. J.* 804, 88. doi:10.1088/0004-637X/804/2/88
- Trottet, G. (1986). Relative timing of hard X-rays and radio emissions during the different phases of solar flares - consequences for the electron acceleration. *Sol. Phys.* 104, 145–163. doi:10.1007/BF00159956
- Tylka, A., and Dietrich, W. (2009). “A new and comprehensive analysis of proton spectra in ground-level enhanced (GLE) solar particle events,” in 31st international cosmic ray conference. Lodz, Poland, 7–15 July 2009. Editor M. Giller, et al. <http://icrc2009.uni.lodz.pl/proc/pdf/icrc0273.pdf>.
- Vainio, R., and Khan, J. I. (2004). Solar energetic particle acceleration in refracting coronal shock waves. *Astrophys. J.* 600, 451–457.
- Vashenyuk, E. V., Balabin, Y. V., Perez-Peraza, J., Gallegos-Cruz, A., and Miroshnichenko, L. I. (2006). Some features of the sources of relativistic particles at the Sun in the solar cycles 21–23. *Adv. Space Res.* 38, 411–417. doi:10.1016/j.asr.2005.05.012
- Vršnak, B., Aurass, H., Magdalenic, J., and Gopalswamy, N. (2001). Band-splitting of coronal and interplanetary type II bursts. I. Basic properties. *Astron. Astrophys.* 377, 321–329. doi:10.1051/0004-6361
- Vršnak, B., and Cliver, E. W. (2008). Origin of coronal shock waves. *Sol. Phys.* 253, 215–235. doi:10.1007/s11207-008-9241-5
- Vršnak, B., Magdalenic, J., Aurass, H., and Mann, G. (2002). Band-splitting of coronal and interplanetary type II bursts. II. Coronal magnetic field and Alfvén velocity. *Astron. Astrophys.* 396, 673–682. doi:10.1051/0004-6361:20021413
- Vršnak, B., Sudar, D., and Ruždjak, D. (2005). The CME-flare relationship: are there really two types of CMEs?. *Astron. Astrophys.* 435, 1149–1157. doi:10.1051/0004-6361:20042166
- Warmuth, A. (2015). Large-scale globally propagating coronal waves. *Living Rev. Sol. Phys.* 12, 1. doi:10.12942/lrsp-2015-3
- Warmuth, A., and Mann, G. (2005). A model of the Alfvén speed in the solar corona. *Astron. Astrophys.* 435, 1123–1135. doi:10.1051/0004-6361:20042169
- Warmuth, A., Vršnak, B., Magdalenic, J., Hanslmeier, A., and Otruba, W. (2004). A multiwavelength study of solar flare waves. II. Perturbation characteristics and physical interpretation. *Astron. Astrophys.* 418, 1117–1129. doi:10.1051/0004-6361:20034333
- Warren, H. P., Brooks, D. H., Ugarte-Urra, I., Reep, J. W., Crump, N. A., and Doschek, G. A. (2018). Spectroscopic observations of current sheet formation and evolution. *Astrophys. J.* 854, 122. doi:10.3847/1538-4357/aaa9b8
- Wild, J. P., Smerd, S. F., and Weiss, A. A. (1963). Solar bursts. *Annu. Rev. Astron. Astrophys.* 1, 291–366. doi:10.1146/annurev.aa.01.090163.001451
- Winter, L. M., and Ledbetter, K. (2015). Type II and type III radio bursts and their correlation with solar energetic proton events. *Astrophys. J.* 809, 105. doi:10.1088/0004-637X/809/1/105
- Yan, X. L., Yang, L. H., Xue, Z. K., Mei, Z. X., Kong, D. F., Wang, J. C., et al. (2018). Simultaneous observation of a flux rope eruption and magnetic reconnection during an X-class solar flare. *Astrophys. J. Lett.* 853, L18. doi:10.3847/2041-8213/aaa6c2
- Yashiro, S., Gopalswamy, N., Michalek, G., Cyr, St. O. C., Plunkett, S. P., Rich, N. B., et al. (2004). A catalog of white light coronal mass ejections observed by the SOHO spacecraft. *J. Geophys. Res.* 109, A07105. doi:10.1029/2003JA010282
- Zimovets, I., Vilmer, N., Chian, A. C.-L., Sharykin, I., and Struminsky, A. (2012). Spatially resolved observations of a split-band coronal type II radio burst. *Astron. Astrophys.* 547, A6. doi:10.1051/0004-6361/201219454
- Zucca, P., Morosan, D. E., Rouillard, A. P., Fallows, R., Gallagher, P. T., Magdalenic, J., et al. (2018). Shock location and CME 3D reconstruction of a solar type II radio burst with LOFAR. *Astron. Astrophys.* 615, A89. doi:10.1051/0004-6361/201732308

Conflict of Interest: The author declares that the research was conducted in the absence of any commercial or financial relationships that could be construed as a potential conflict of interest.

Copyright © 2021 Klein. This is an open-access article distributed under the terms of the Creative Commons Attribution License (CC BY). The use, distribution or reproduction in other forums is permitted, provided the original author(s) and the copyright owner(s) are credited and that the original publication in this journal is cited, in accordance with accepted academic practice. No use, distribution or reproduction is permitted which does not comply with these terms.